A Unified Framework for Optimizing Linear Nonregenerative Multicarrier MIMO Relay Communication Systems

Yue Rong, *Member, IEEE*, Xiaojun Tang, *Student Member, IEEE*, and Yingbo Hua, *Fellow, IEEE*

***Abstract*—In this paper, we develop a unified framework for linear nonregenerative multicarrier multiple-input multiple-output (MIMO) relay communications in the absence of the direct source–destination link. This unified framework classifies most commonly used design objectives such as the minimal mean-square error and the maximal mutual information into two categories: Schur-concave and Schur-convex functions. We prove that for Schur-concave objective functions, the optimal source precoding matrix and relay amplifying matrix jointly diagonalize the source–relay–destination channel matrix and convert the multicarrier MIMO relay channel into parallel single-input single-output (SISO) relay channels. While for Schur-convex objectives, such joint diagonalization occurs after a specific rotation of the source precoding matrix. After the optimal structure of the source and relay matrices is determined, the linear nonregenerative relay design problem boils down to the issue of power loading among the resulting SISO relay channels. We show that this power loading problem can be efficiently solved by an alternating technique. Numerical examples demonstrate the effectiveness of the proposed framework.**

***Index Terms*—Majorization, MIMO relay, multicarrier system, nonregenerative relay.**

I. Introduction

Research on cooperative communications employing relay nodes dates back to 1970s [1], [2]. Recently, cooperative communications have seen a renewed interest [3]–[6]. Both regenerative and nonregenerative cooperative strategies have been considered [3]–[6]. When multiple antennas are deployed at one or more nodes of the relay system, we also call such relay system a multiple-input multiple-output (MIMO) relay channel. The achievable rate and capacity upper bound of a MIMO relay channel have been studied in [7]. The diversity-multiplexing tradeoff of multiantenna cooperative systems has been studied in [8].

Manuscript received December 09, 2008; accepted June 19, 2009. First published July 14, 2009; current version published November 18, 2009. The associate editor coordinating the review of this manuscript and approving it for publication was Prof. Athanasios P. Liavas. The work of Y. Hua is supported in part by the U.S. Army Research Office under the MURI Grant W911NF-04-1-0224, and the U.S. National Science Foundation under Grant TF-0514736.

Y. Rong is with the Department of Electrical and Computer Engineering, Curtin University of Technology, Bentley, WA 6102, Australia (e-mail: y.rong@curtin.edu.au).

X. Tang is with the WINLAB, Rutgers University, North Brunswick, NJ 08902 USA (e-mail: xtang@winlab.rutgers.edu).

Y. Hua is with the Department of Electrical Engineering, University of California, Riverside, CA 92521 USA (e-mail: yhua@ee.ucr.edu).

Digital Object Identifier 10.1109/TSP.2009.2027779

For the nonregenerative strategy, the relay node only amplifies and retransmits its received signal. The complexity of the nonregenerative strategy is much lower than that of the regenerative strategy. This advantage is particularly important when all nodes are equipped with multiple antennas, since decoding multiple data streams involves much more computational efforts than decoding a single data stream.

Linear nonregenerative approaches have been proposed for single carrier MIMO relay systems [9]–[13]. In [9], the optimal relay amplifying matrix which maximizes the mutual information (MI) between source and destination was derived assuming that the source covariance matrix is an identity matrix. This approach is suitable when the source-relay channel state information (CSI) is unknown to the scheduler. Independent from [9], the authors of [10] also studied a similar problem and arrived at the same optimal relay amplifying matrix. In [11], both the source covariance matrix and the relay amplifying matrix are jointly designed to maximize the source-destination MI. This approach requires the scheduler to know all CSI of the relay system, which we also assume in this paper. Minimal arithmetic mean-square error (MA-MSE)-based approaches for MIMO relay systems were developed in [12], [13]. A method based on maximum signal-to-noise ratio (SNR) was proposed by the authors of [13]. In [14], the authors compared the performance-complexity tradeoffs of nonregenerative and other MIMO relay techniques. Examples of recent work on multicarrier MIMO relay systems are in [15] and [16]. The design criterion in [15] is to maximize the source-destination MI. The work in [16] aims to minimize the arithmetic sum of the MSE of the signal waveform estimation at all data streams. While the above works [9]–[16] assume complete CSI, another line of research on nonregenerative MIMO relaying assumes partial CSI [17], [18]. In the sequel, for simplicity, we refer to the source precoding matrix and relay amplifying matrix as source matrix and relay matrix, respectively.

A key component in linear nonregenerative MIMO relay design is to optimize the source and relay matrices to maximize (minimize) an objective function. In this paper, we consider the design of a linear nonregenerative multicarrier MIMO relay system under a unified framework that is more general than those used in [9]–[16]. We focus on the case where the direct link between the source and destination nodes is sufficiently weak to be ignored as in [11]–[13] and [15]. This scenario occurs when the direct link is blocked by an obstacle such as a mountain. Our unified framework classifies most common design objectives such as the maximal MI, minimal MSE, and minimax MSE, etc., into two broad categories: Schur-convex and Schur-concave functions of the main diagonal elements of the MSE matrix. By using the theory of majorization [19], [20], we prove that for Schur-concave objective functions, the optimal source and relay matrices jointly diagonalize the source-relay-destination channel, and convert the multicarrier MIMO relay channel into parallel single-input single-output (SISO) relay channels. While for Schur-convex objectives, such a joint channel diagonalization occurs after a specific rotation of the source matrix. Note that for one-hop MIMO systems (either single-user or multiuser systems), the optimality of channel diagonalization has been proven in [21]–[23]. For linear MIMO relay systems, the channel diagonalization optimality has been shown under the maximal MI objective [9]–[11] and the MA-MSE criterion [12], [13]. However, the channel diagonalization optimality results obtained in this paper are more general, since they include *all* Schur-concave and Schur-convex objective functions.

After the optimal structure of the source and relay matrices is determined, the linear nonregenerative multicarrier MIMO relay design problems boil down to the issues of power loading among the resulting SISO relay channels based on the given criterion. We demonstrate that the power loading problem can be efficiently solved by iteratively updating the power allocation vectors at the source and relay nodes [11], [15], [16]. Interestingly, the updating of each power allocation vector follows the well-known water-filling principle for Schur-concave objectives. While for Schur-convex functions, the power allocation result can be viewed as a multilevel water-filling solution. Numerical examples in Section IV illustrate the effectiveness of the proposed framework.

The main contributions of this paper are summarized as follows: First, we rigorously prove the optimality of channel diagonalization in nonregenerative multicarrier MIMO relay systems. As the second contribution, we propose a novel MIMO relaying algorithm based on Schur-convex objective function. Note that there is no existing work in nonregenerative MIMO relay communication area which addresses Schur-convex objective functions. It will be seen that the new algorithm has a much better performance in terms of raw bit-error-rate (BER) and clipping probability than all competing algorithms. For the third contribution, we investigate the performance-complexity tradeoff of subcarrier-independent and subcarrier-cooperative nonregenerative MIMO relay systems. We show that a subcarrier-independent system trades only a slight performance loss for a much reduced computational complexity and thus is very attractive for practical applications.

We would like to mention that majorization theory has been applied for optimizing the source matrix in a point-to-point multicarrier MIMO system [21]. In fact, a point-to-point MIMO system can be viewed as a special case of a linear MIMO relay system, where either the source-relay link or the relay-destination link has a very high (infinite) channel gain. Thus, our work is a generalization of the results in [21]. In [24], the authors applied majorization theory to optimize the relay matrices in the asymptotic regime of a multilevel nonregenerative relay channel.

Compared with the point-to-point MIMO system [21], the objective function of MIMO relay systems depends on both the source and relay matrices. Moreover, the additional constraint on the transmission power at the relay node is a function of both the source and relay matrices. Therefore, although both [21] and our work apply the majorization theory to prove the optimality of channel diagonalization, it will be seen that the introduction of the relay node greatly complicates the proof. A rigorous proof of the main theorem in this paper is technically challenging. In fact, the only part in [21] that is used in the current work is the link between some practical objective functions and the main diagonal elements of the minimal MSE matrix.

The rest of this paper is organized as follows. In Section II we introduce the system model for a three-node linear nonregenerative multicarrier MIMO relay communication system. The proposed framework is developed in Section III. In Section IV, we show some numerical examples. Conclusions are drawn in Section V.

II. System Model

We consider a three-node multicarrier MIMO communication system where the source node transmits information to the destination node with the aid of one relay node. The source, relay, and destination nodes are equipped with N_s, N_r, and N_d antennas, respectively. To account for the practical half-duplex constraint that a node cannot transmit and receive at the same time within the same spectrum band, we assume that the source-relay and relay-destination channels are orthogonal. To efficiently exploit the system hardware, the relay node uses the same antennas to transmit and receive signals. Due to its merit of simplicity, a linear nonregenerative strategy is applied at the relay node to process and forward the received signal.

We use the (either physical or virtual) multicarrier technique to turn a broadband frequency-selective channel into multiple frequency-flat subcarrier channels. Based on whether the subcarriers cooperate with each other in processing the signals at the source and relay nodes, we can have either subcarrier-independent or subcarrier-cooperative systems.

A. Subcarrier-Independent System

The communication process between the source and destination nodes is completed in two time slots. In the first slot, the modulated signal sequence at the source node is divided into N_c blocks. We denote $N_b^{[n]}$, $n = 1, \ldots, N_c$, as the number of symbols in the nth subblock. Hereafter, the superscript $[n]$ denotes the corresponding variables for the nth subcarrier. The $N_b^{[n]} \times 1$ symbol vector $\mathbf{s}^{[n]}(t)$ is linearly precoded as

$$\mathbf{x}^{[n]}(t) = \mathbf{B}^{[n]}\mathbf{s}^{[n]}(t), \quad n = 1, \ldots, N_c$$

where $\mathbf{B}^{[n]}$ is an $N_s \times N_b^{[n]}$, $\left(N_s \geq N_b^{[n]}\right)$ source precoding matrix for the nth subblock of the source symbol sequence. The precoded vector $\mathbf{x}^{[n]}(t)$ is transmitted to the relay node via the nth subcarrier. The received signal at the relay node can be written as

$$\mathbf{y}_r^{[n]}(t) = \mathbf{H}_{sr}^{[n]}\mathbf{x}^{[n]}(t) + \mathbf{v}_r^{[n]}(t), \quad n = 1, \ldots, N_c$$

where $\mathbf{H}_{sr}^{[n]}$ is an $N_r \times N_s$ MIMO channel matrix between the source and relay nodes, $\mathbf{y}_r^{[n]}(t)$ and $\mathbf{v}_r^{[n]}(t)$ are the received signal and the additive Gaussian noise vectors at the relay node, respectively.

In the second slot, the source node is silent and the relay node multiplies (linearly precodes) the received signal vector at the nth subcarrier by an $N_r \times N_r$ relay amplifying matrix $\mathbf{F}^{[n]}$ and transmits the precoded signal vector

$$\mathbf{x}_r^{[n]}(t+1) = \mathbf{F}^{[n]}\mathbf{y}_r^{[n]}(t), \quad n = 1, \ldots, N_c$$

to the destination node. The received signal vector at the nth subcarrier of the destination node can be written as

$$\begin{aligned}\mathbf{y}_d^{[n]}(t+1) &= \mathbf{H}_{rd}^{[n]}\mathbf{x}_r^{[n]}(t+1) + \mathbf{v}_d^{[n]}(t+1)\\ &= \mathbf{H}_{rd}^{[n]}\mathbf{F}^{[n]}\mathbf{H}_{sr}^{[n]}\mathbf{B}^{[n]}\mathbf{s}^{[n]}(t)\\ &\quad + \mathbf{H}_{rd}^{[n]}\mathbf{F}^{[n]}\mathbf{v}_r^{[n]}(t)\\ &\quad + \mathbf{v}_d^{[n]}(t+1) \quad n = 1, \ldots, N_c \end{aligned} \tag{1}$$

where $\mathbf{H}_{rd}^{[n]}$ is an $N_d \times N_r$ MIMO channel matrix between the relay and destination nodes, $\mathbf{y}_d^{[n]}(t+1)$ and $\mathbf{v}_d^{[n]}(t+1)$ are the received signal and the additive Gaussian noise vectors at the destination node, respectively. We assume that $\mathbf{H}_{sr}^{[n]}$ and $\mathbf{H}_{rd}^{[n]}$, $n = 1, \ldots, N_c$, are all quasi-static and known by the scheduler and the destination node. The source and relay matrices are calculates by the scheduler, which can be any node in the system. The optimal $\mathbf{B}^{[n]}$ is forwarded from the scheduler to the source and destination nodes, while $\mathbf{F}^{[n]}$ is sent to the relay and destination nodes. We assume that without wasting the transmission power at the source and relay nodes, $N_b^{[n]} \leq \min\left(\mathrm{rank}\left(\mathbf{H}_{sr}^{[n]}\right), \mathrm{rank}\left(\mathbf{H}_{rd}^{[n]}\right)\right)$ and $\mathrm{rank}(\mathbf{F}^{[n]}) = \mathrm{rank}(\mathbf{B}^{[n]}) = N_b^{[n]}$, where $\mathrm{rank}(\cdot)$ stands for the rank of a matrix.

Note that if the noise vectors are spatially correlated such that $\mathbf{C}_r^{[n]} \triangleq \mathrm{E}\left[\mathbf{v}_r^{[n]}(t)\left(\mathbf{v}_r^{[n]}(t)\right)^H\right] \neq \mathbf{I}_{N_r}$ and/or $\mathbf{C}_d^{[n]} \triangleq \mathrm{E}\left[\mathbf{v}_d^{[n]}(t)\left(\mathbf{v}_d^{[n]}(t)\right)^H\right] \neq \mathbf{I}_{N_d}$, pre-whitening of the received signals can be performed at the relay and destination nodes such that

$$\begin{aligned}\tilde{\mathbf{y}}_d^{[n]}(t+1) &= \tilde{\mathbf{H}}_{rd}^{[n]}\tilde{\mathbf{F}}^{[n]}\tilde{\mathbf{H}}_{sr}^{[n]}\mathbf{B}^{[n]}\mathbf{s}^{[n]}(t)\\ &\quad + \tilde{\mathbf{H}}_{rd}^{[n]}\tilde{\mathbf{F}}^{[n]}\tilde{\mathbf{v}}_r^{[n]}(t) + \tilde{\mathbf{v}}_d^{[n]}(t+1), \quad n = 1, \ldots, N_c \end{aligned} \tag{2}$$

where $\mathbf{I}_n$ denotes an $n \times n$ identity matrix, $\mathrm{E}[\cdot]$ stands for the statistical expectation, $(\cdot)^H$ denotes the matrix (vector) Hermitian transpose, and

$$\begin{aligned}\tilde{\mathbf{H}}_{sr}^{[n]} &= \left(\mathbf{C}_r^{[n]}\right)^{-1/2}\mathbf{H}_{sr}^{[n]}\\ \tilde{\mathbf{v}}_r^{[n]}(t) &= \left(\mathbf{C}_r^{[n]}\right)^{-1/2}\mathbf{v}_r^{[n]}(t)\\ \tilde{\mathbf{F}}^{[n]} &= \mathbf{F}^{[n]}\left(\mathbf{C}_r^{[n]}\right)^{1/2}\\ \tilde{\mathbf{y}}_d^{[n]}(t+1) &= \left(\mathbf{C}_d^{[n]}\right)^{-1/2}\mathbf{y}_d^{[n]}(t+1)\\ \tilde{\mathbf{H}}_{rd}^{[n]} &= \left(\mathbf{C}_d^{[n]}\right)^{-1/2}\mathbf{H}_{rd}^{[n]}\\ \tilde{\mathbf{v}}_d^{[n]}(t+1) &= \left(\mathbf{C}_d^{[n]}\right)^{-1/2}\mathbf{v}_d^{[n]}(t+1).\end{aligned}$$

From (2) we see that all noises are independent and identically distributed (i.i.d.). Thus, in the following, without loss of generality, we assume i.i.d. complex circularly symmetric Gaussian noise with zero mean and unit variance, and use (1) as the system input-output model for subcarrier-independent systems.

It is worth noting that the subcarrier-independent system model can also be used for two-hop MIMO relay systems with multiple MIMO relay nodes when the relay nodes do not cooperate with each other and the signals at different source-relay-destination links are transmitted at orthogonal time/frequency slots.

B. Subcarrier-Cooperative System

The input-output model for a subcarrier-cooperative MIMO relay communication system is

$$\mathbf{y}_d(t+1) = \mathbf{H}_{rd}\mathbf{F}\mathbf{H}_{sr}\mathbf{B}\mathbf{s}(t) + \mathbf{H}_{rd}\mathbf{F}\mathbf{v}_r(t) + \mathbf{v}_d(t+1) \tag{3}$$

where

$$\mathbf{H}_{sr} = \mathrm{bd}\left(\mathbf{H}_{sr}^{[1]}, \mathbf{H}_{sr}^{[2]}, \ldots, \mathbf{H}_{sr}^{[N_c]}\right) \tag{4}$$

$$\mathbf{H}_{rd} = \mathrm{bd}\left(\mathbf{H}_{rd}^{[1]}, \mathbf{H}_{rd}^{[2]}, \ldots, \mathbf{H}_{rd}^{[N_c]}\right) \tag{5}$$

$$\begin{aligned}\mathbf{s}(t) &= \left[\left(\mathbf{s}^{[1]}(t)\right)^T, \left(\mathbf{s}^{[2]}(t)\right)^T, \ldots, \left(\mathbf{s}^{[N_c]}(t)\right)^T\right]^T\\ \mathbf{v}_r(t) &= \left[\left(\mathbf{v}_r^{[1]}(t)\right)^T, \left(\mathbf{v}_r^{[2]}(t)\right)^T, \ldots, \left(\mathbf{v}_r^{[N_c]}(t)\right)^T\right]^T\\ \mathbf{v}_d(t+1) &= \left[\left(\mathbf{v}_d^{[1]}(t+1)\right)^T, \left(\mathbf{v}_d^{[2]}(t+1)\right)^T, \ldots, \right.\\ &\qquad \left.\left(\mathbf{v}_d^{[N_c]}(t+1)\right)^T\right]^T\\ \mathbf{y}_d(t+1) &= \left[\left(\mathbf{y}_d^{[1]}(t+1)\right)^T, \left(\mathbf{y}_d^{[2]}(t+1)\right)^T, \ldots, \right.\\ &\qquad \left.\left(\mathbf{y}_d^{[N_c]}(t+1)\right)^T\right]^T.\end{aligned}$$

Here $(\cdot)^T$ denotes the matrix (vector) transpose, $\mathrm{bd}(\cdot)$ stands for a block-diagonal matrix, $\mathbf{H}_{sr}$ is an $N_cN_r \times N_cN_s$ block-diagonal matrix of the "super" channel of the source-relay link, $\mathbf{H}_{rd}$ is an $N_cN_d \times N_cN_r$ block-diagonal "super" channel matrix between the relay and destination nodes, $\mathbf{s}(t)$, $\mathbf{v}_r(t)$, $\mathbf{v}_d(t+1)$, and $\mathbf{y}_d(t+1)$ are obtained by stacking the corresponding vectors at all subcarriers. From (3), we see that the cooperation among different subcarriers is performed by a "super" $N_cN_s \times L$ source matrix $\mathbf{B}$ where $L \triangleq \sum_{n=1}^{N_c} N_b^{[n]}$, and a "super" relay matrix $\mathbf{F}$ with a dimension of $N_cN_r \times N_cN_r$.

A subcarrier-cooperative MIMO relay system is a generalization of a subcarrier-independent system, since if we impose a block-diagonal structure on both $\mathbf{F}$ and $\mathbf{B}$ such that

$$\begin{aligned}\mathbf{F} &= \mathrm{bd}\left(\mathbf{F}^{[1]}, \mathbf{F}^{[2]}, \ldots, \mathbf{F}^{[N_c]}\right)\\ \mathbf{B} &= \mathrm{bd}\left(\mathbf{B}^{[1]}, \mathbf{B}^{[2]}, \ldots, \mathbf{B}^{[N_c]}\right)\end{aligned}$$

then (3) becomes (1). Hence, we anticipate that a subcarrier-cooperative system has a better performance than a subcarrier-independent system. Interestingly, from a mathematical point of view, the subcarrier-independent system model (1) is more general, since (3) can be obtained from (1) by simply setting $N_c = 1$. Thus, in the following, we use (1) to develop the unified framework. After the establishment of the unified framework, we revisit (3) to derive the optimal structure of $\mathbf{F}$ and $\mathbf{B}$ for subcarrier-cooperative systems.

III. Proposed Unified Framework

In this section, we develop a unified framework for most common linear nonregenerative multicarrier MIMO relay design problems.

First we establish the link between the main diagonal elements of the minimal MSE matrix and various common design objectives. Using a linear receiver, the estimated signal waveform at the destination node is given by

$$\hat{\mathbf{s}}^{[n]}(t) = \left(\mathbf{W}^{[n]}\right)^H \mathbf{y}_d^{[n]}(t+1), \quad n = 1,\ldots,N_c$$

where $\mathbf{W}^{[n]}$ is an $N_d \times N_b^{[n]}$ weight matrix at the nth subcarrier. The MSE matrix at the nth subcarrier of the destination node is given by

$$\begin{aligned}\mathbf{E}^{[n]} &\triangleq \mathrm{E}\left[\left(\hat{\mathbf{s}}^{[n]}(t) - \mathbf{s}^{[n]}(t)\right)\left(\hat{\mathbf{s}}^{[n]}(t) - \mathbf{s}^{[n]}(t)\right)^H\right] \\ &= \left(\mathbf{W}^{[n]}\bar{\mathbf{H}}^{[n]} - \mathbf{I}_{N_b^{[n]}}\right)\left(\mathbf{W}^{[n]}\bar{\mathbf{H}}^{[n]} - \mathbf{I}_{N_b^{[n]}}\right)^H \\ &\quad + \left(\mathbf{W}^{[n]}\right)^H \bar{\mathbf{C}}^{[n]}\mathbf{W}^{[n]}, \quad n = 1,\ldots,N_c \qquad (6)\end{aligned}$$

where we assume that $\mathrm{E}\left[\mathbf{s}^{[n]}(t)\left(\mathbf{s}^{[n]}(t)\right)^H\right] = \mathbf{I}_{N_b^{[n]}}$, $\bar{\mathbf{H}}^{[n]}$ is the effective MIMO channel matrix of the source-relay-destination link, and $\bar{\mathbf{C}}^{[n]}$ is the equivalent noise covariance matrix. They are written respectively as

$$\begin{aligned}\bar{\mathbf{H}}^{[n]} &\triangleq \mathbf{H}_{rd}^{[n]}\mathbf{F}^{[n]}\mathbf{H}_{sr}^{[n]}\mathbf{B}^{[n]} \\ \bar{\mathbf{C}}^{[n]} &\triangleq \mathbf{H}_{rd}^{[n]}\mathbf{F}^{[n]}(\mathbf{F}^{[n]})^H\left(\mathbf{H}_{rd}^{[n]}\right)^H + \mathbf{I}_{N_d}.\end{aligned}$$

The weight matrix of the optimal linear receiver which minimizes $\mathbf{E}^{[n]}$ is the Wiener filter given by [25]

$$\mathbf{W}_0^{[n]} = \left(\bar{\mathbf{H}}^{[n]}\left(\bar{\mathbf{H}}^{[n]}\right)^H + \bar{\mathbf{C}}^{[n]}\right)^{-1}\bar{\mathbf{H}}^{[n]}, \quad n = 1,\ldots,N_c \qquad (7)$$

where $(\cdot)^{-1}$ denotes the matrix inversion. Here for matrix variables, $\mathbf{E}^{[n]}\left(\mathbf{W}_0^{[n]}\right)$ is minimal indicates that $\mathbf{E}^{[n]}\left(\mathbf{W}^{[n]}\right) - \mathbf{E}^{[n]}\left(\mathbf{W}_0^{[n]}\right)$ is a positive semi-definite matrix for any $\mathbf{W}^{[n]} \neq \mathbf{W}_0^{[n]}$. Substituting (7) back into (6), we find that the minimal MSE matrix is a function of $\mathbf{B}^{[n]}$ and $\mathbf{F}^{[n]}$ and can be written as

$$\begin{aligned}&\mathbf{E}_0^{[n]}\left(\mathbf{B}^{[n]},\mathbf{F}^{[n]}\right) \\ &= \left[\mathbf{I}_{N_b^{[n]}} + \left(\bar{\mathbf{H}}^{[n]}\right)^H\left(\bar{\mathbf{C}}^{[n]}\right)^{-1}\bar{\mathbf{H}}^{[n]}\right]^{-1} n = 1,\ldots,N_c. \qquad (8)\end{aligned}$$

The link between most practical objective functions and the main diagonal elements of the minimal MSE matrix has been established in [21] for point-to-point multicarrier MIMO communications. Now we show that such link can be extended to linear nonregenerative multicarrier MIMO relay communications. We take as examples three common functions: the arithmetic sum of the MSE (AMSE) of the signal waveform estimation at all data streams, the MI between source and destination, and the geometric product of the signal-to-interference-noise ratio (SINR) of all data streams. First, AMSE can be written as

$$\begin{aligned}&\mathrm{AMSE}\left(\{\mathbf{B}^{[n]}\},\{\mathbf{F}^{[n]}\}\right) \\ &= \sum_{n=1}^{N_c}\mathrm{tr}\left(\left[\mathbf{I}_{N_b^{[n]}} + \left(\bar{\mathbf{H}}^{[n]}\right)^H\left(\bar{\mathbf{C}}^{[n]}\right)^{-1}\bar{\mathbf{H}}^{[n]}\right]^{-1}\right) \\ &= \sum_{n=1}^{N_c}\sum_{i=1}^{N_b^{[n]}}\left[\mathbf{E}_0^{[n]}\left(\mathbf{B}^{[n]},\mathbf{F}^{[n]}\right)\right]_{i,i} \qquad (9)\end{aligned}$$

where for a matrix $\mathbf{A}$, $\{\mathbf{A}^{[n]}\} \triangleq \{\mathbf{A}^{[1]},\mathbf{A}^{[2]},\ldots,\mathbf{A}^{[N_c]}\}$, $[\mathbf{A}]_{i,j}$ denotes the (i,j)-th element of $\mathbf{A}$, and $\mathrm{tr}(\mathbf{A})$ stands for the trace of $\mathbf{A}$. Here $\left[\mathbf{E}_0^{[n]}\left(\mathbf{B}^{[n]},\mathbf{F}^{[n]}\right)\right]_{i,i}$ is the MSE of the signal waveform estimation of the ith data stream at the nth subcarrier, given by

$$\left[\mathbf{E}_0^{[n]}\left(\mathbf{B}^{[n]},\mathbf{F}^{[n]}\right)\right]_{i,i} = \left[1 + \left(\bar{\mathbf{h}}_i^{[n]}\right)^H\mathbf{C}_i^{[n]}\bar{\mathbf{h}}_i^{[n]}\right]^{-1}$$

where $\bar{\mathbf{h}}_i^{[n]}$ is the ith column vector of $\bar{\mathbf{H}}^{[n]}$, and $\mathbf{C}_i^{[n]} = \bar{\mathbf{C}}^{[n]} + \bar{\mathbf{H}}^{[n]}\left(\bar{\mathbf{H}}^{[n]}\right)^H - \bar{\mathbf{h}}_i^{[n]}\left(\bar{\mathbf{h}}_i^{[n]}\right)^H$ is the interference-plus-noise covariance matrix for the ith data stream at the nth subcarrier.

Second, the MI between source and destination is

$$\begin{aligned}&\mathrm{MI}\left(\{\mathbf{B}^{[n]}\},\{\mathbf{F}^{[n]}\}\right) \\ &\qquad = \sum_{n=1}^{N_c}\log_2\left|\mathbf{I}_{N_b^{[n]}} + \left(\bar{\mathbf{H}}^{[n]}\right)^H\left(\bar{\mathbf{C}}^{[n]}\right)^{-1}\bar{\mathbf{H}}^{[n]}\right| \qquad (10)\end{aligned}$$

where $|\cdot|$ denotes the matrix determinant. Since (10) is invariant to any unitary rotation of $\mathbf{B}^{[n]}$, we choose $\mathbf{B}^{[n]}$ such that $\left(\bar{\mathbf{H}}^{[n]}\right)^H\left(\bar{\mathbf{C}}^{[n]}\right)^{-1}\bar{\mathbf{H}}^{[n]}$, $n = 1,\ldots,N_c$ is diagonal. Thus, we have

$$\mathrm{MI}\left(\{\mathbf{B}^{[n]}\},\{\mathbf{F}^{[n]}\}\right) = -\sum_{n=1}^{N_c}\sum_{i=1}^{N_b^{[n]}}\log_2\left[\mathbf{E}_0^{[n]}\left(\mathbf{B}^{[n]},\mathbf{F}^{[n]}\right)\right]_{i,i}. \qquad (11)$$

Finally, the geometric product of the SINR of all data streams is given by

$$\begin{aligned}\mathrm{SINR}\left(\mathbf{B}^{[n]},\mathbf{F}^{[n]}\right) &= \prod_{n=1}^{N_c}\prod_{i=1}^{N_b^{[n]}}\left(\bar{\mathbf{h}}_i^{[n]}\right)^H\left(\mathbf{C}_i^{[n]}\right)^{-1}\bar{\mathbf{h}}_i^{[n]} \\ &= \prod_{n=1}^{N_c}\prod_{i=1}^{N_b^{[n]}}\left(\frac{1}{\left[\mathbf{E}_0^{[n]}(\mathbf{B}^{[n]},\mathbf{F}^{[n]})\right]_{i,i}} - 1\right). \qquad (12)\end{aligned}$$

From (9), (11), and (12) we see that all three functions are strongly linked to the main diagonal elements of $\mathbf{E}_0^{[n]}\left(\mathbf{B}^{[n]},\mathbf{F}^{[n]}\right)$, $n = 1,\ldots,N_c$. Let us use $f\left(\mathbf{d}\left[\mathbf{E}_0^{[n]}\left(\mathbf{B}^{[n]},\mathbf{F}^{[n]}\right)\right]\right)$ as a unified notation for the objective function at the nth subcarrier, where $\mathbf{d}[\mathbf{A}]$ is a column vector containing all main diagonal elements of $\mathbf{A}$. Then at the nth subcarrier, the linear nonregenerative multicarrier MIMO relay design problem can be written as

$$\min_{\mathbf{B}^{[n]},\mathbf{F}^{[n]}} \quad f\left(\mathbf{d}\left[\mathbf{E}_0^{[n]}\left(\mathbf{B}^{[n]},\mathbf{F}^{[n]}\right)\right]\right) \tag{13}$$

$$\text{s.t.} \quad \mathrm{tr}\left(\mathbf{B}^{[n]}\left(\mathbf{B}^{[n]}\right)^H\right) \le p_s^{[n]} \tag{14}$$

$$\mathrm{tr}\Bigg(\mathbf{F}^{[n]}\left[\mathbf{H}_{sr}^{[n]}\mathbf{B}^{[n]}\left(\mathbf{B}^{[n]}\right)^H\left(\mathbf{H}_{sr}^{[n]}\right)^H + \mathbf{I}_{N_r}\right]\left(\mathbf{F}^{[n]}\right)^H\Bigg) \le p_r^{[n]} \tag{15}$$

where (14) and (15) are constraints for the transmission power at the source and relay nodes, respectively. Here $p_s^{[n]} \ge 0$ and $p_r^{[n]} \ge 0$ are the corresponding power used at the nth subcarrier satisfying $\sum_{n=1}^{N_c} p_s^{[n]} \le p_s$ and $\sum_{n=1}^{N_c} p_r^{[n]} \le p_r$. We denote p_s and p_r as the total power constraints across all subcarriers at the source and relay nodes, respectively.

Before stating the key theorem on the solution of problem (13)–(15), we introduce two important definitions from [19].

Definition 1 [19, 1.A.1, 1.A.2]: Consider any two real-valued $N \times 1$ vectors $\mathbf{x}$ and $\mathbf{y}$, let $x_{[1]} \ge x_{[2]} \ge \cdots \ge x_{[N]}$, $y_{[1]} \ge y_{[2]} \ge \cdots \ge y_{[N]}$ denote the elements of $\mathbf{x}$ and $\mathbf{y}$ sorted in decreasing order, respectively. Then we say that $\mathbf{x}$ is majorized by $\mathbf{y}$, or $\mathbf{x} \prec \mathbf{y}$, if $\sum_{i=1}^{n} x_{[i]} \le \sum_{i=1}^{n} y_{[i]}$, for $n = 1,\ldots,N-1$, and $\sum_{i=1}^{N} x_{[i]} = \sum_{i=1}^{N} y_{[i]}$. Vector $\mathbf{x}$ is weakly submajorized by vector $\mathbf{y}$, or $\mathbf{x} \prec_{\mathrm{w}} \mathbf{y}$, if $\sum_{i=1}^{n} x_{[i]} \le \sum_{i=1}^{n} y_{[i]}$, for $n = 1,\ldots,N$.

Definition 2 [19, 3.A.1]: A real-valued function f is Schur-convex if for $\mathbf{x} \prec \mathbf{y}$, there is $f(\mathbf{x}) \le f(\mathbf{y})$. Similarly, f is Schur-concave if $f(\mathbf{x}) \ge f(\mathbf{y})$, for $\mathbf{x} \prec \mathbf{y}$.

Let us denote

$$\mathbf{H}_{sr}^{[n]} \triangleq \mathbf{U}_s^{[n]}\mathbf{\Lambda}_s^{[n]}\left(\mathbf{V}_s^{[n]}\right)^H \tag{16}$$

$$\mathbf{H}_{rd}^{[n]} \triangleq \mathbf{U}_r^{[n]}\mathbf{\Lambda}_r^{[n]}\left(\mathbf{V}_r^{[n]}\right)^H \tag{17}$$

as the singular value decomposition (SVD) of $\mathbf{H}_{sr}^{[n]}$ and $\mathbf{H}_{rd}^{[n]}$, where the dimensions of $\mathbf{U}_s^{[n]}, \mathbf{\Lambda}_s^{[n]}, \mathbf{V}_s^{[n]}$ are $N_r \times N_r$, $N_r \times N_s$, $N_s \times N_s$, respectively, and the dimensions of $\mathbf{U}_r^{[n]}, \mathbf{\Lambda}_r^{[n]}, \mathbf{V}_r^{[n]}$ are given as $N_d \times N_d$, $N_d \times N_r$, $N_r \times N_r$, respectively. We assume that the main diagonal elements of $\mathbf{\Lambda}_s^{[n]}$ and $\mathbf{\Lambda}_r^{[n]}$ are arranged in increasing order, respectively. The following theorem is the main contribution of this paper. It establishes the structure of the optimal $\mathbf{B}^{[n]}, \mathbf{F}^{[n]}$ for Schur-concave and Schur-convex objective functions, respectively.

Theorem 1: For the linear nonregenerative multicarrier MIMO relay optimization problem (13)–(15) with an $N_s \times N_b^{[n]}$ matrix $\mathbf{B}^{[n]}$, we assume that i) The objective function in (13) is an increasing function of $\mathbf{d}\left[\mathbf{E}_0^{[n]}\left(\mathbf{B}^{[n]},\mathbf{F}^{[n]}\right)\right]$; ii) $\mathrm{rank}\left(\mathbf{B}^{[n]}\right) = \mathrm{rank}\left(\mathbf{F}^{[n]}\right) = N_b^{[n]} \le \min\left(\mathrm{rank}\left(\mathbf{H}_{sr}^{[n]}\right), \mathrm{rank}\left(\mathbf{H}_{rd}^{[n]}\right)\right)$. If the objective function in (13) is a Schur-concave function of $\mathbf{d}\left[\mathbf{E}_0^{[n]}\left(\mathbf{B}^{[n]},\mathbf{F}^{[n]}\right)\right]$, then the optimal source and relay matrices have the following structure:

$$\mathbf{F}_0^{[n]} = \mathbf{V}_{r,1}^{[n]}\mathbf{\Lambda}_f^{[n]}\left(\mathbf{U}_{s,1}^{[n]}\right)^H \tag{18}$$

$$\mathbf{B}_0^{[n]} = \mathbf{V}_{s,1}^{[n]}\mathbf{\Lambda}_b^{[n]} \tag{19}$$

where $\mathbf{\Lambda}_f^{[n]}$ and $\mathbf{\Lambda}_b^{[n]}$ are $N_b^{[n]} \times N_b^{[n]}$ diagonal matrices, $\mathbf{V}_{r,1}^{[n]}$, $\mathbf{U}_{s,1}^{[n]}$, and $\mathbf{V}_{s,1}^{[n]}$ contain the rightmost $N_b^{[n]}$ columns from $\mathbf{V}_r^{[n]}$, $\mathbf{U}_s^{[n]}$, and $\mathbf{V}_s^{[n]}$, respectively.

On the other hand, if (13) is a Schur-convex function of $\mathbf{d}\left[\mathbf{E}_0^{[n]}\left(\mathbf{B}^{[n]},\mathbf{F}^{[n]}\right)\right]$, $\mathbf{F}_0^{[n]}$ is given by (18), while $\mathbf{B}_0^{[n]}$ has the structure as

$$\mathbf{B}_0^{[n]} = \mathbf{V}_{s,1}^{[n]}\mathbf{\Lambda}_b^{[n]}\mathbf{V}_b^{[n]} \tag{20}$$

where $\mathbf{V}_b^{[n]}$ is an $N_b^{[n]} \times N_b^{[n]}$ unitary (rotation) matrix such that $\mathbf{d}\left[\mathbf{E}_0^{[n]}\left(\mathbf{B}_0^{[n]},\mathbf{F}_0^{[n]}\right)\right]$ has identical elements.

Proof: See the Appendix. □

Condition i) is a natural choice for any practical purpose. While condition ii) sets the upper-bound for the maximal number of independent data streams in each subcarrier such that no transmission power is wasted. From Theorem 1, we see that for Schur-concave objective functions, the optimal relay and source matrices (18) and (19) jointly diagonalize the source-relay-destination channel. The equivalent minimal MSE matrix is diagonal and given by

$$\mathbf{E}_0^{[n]}\left(\mathbf{\Lambda}_f^{[n]},\mathbf{\Lambda}_b^{[n]}\right) = \Bigg[\mathbf{I}_{N_b^{[n]}} + \left(\mathbf{\Lambda}_{r,1}^{[n]}\mathbf{\Lambda}_f^{[n]}\mathbf{\Lambda}_{s,1}^{[n]}\mathbf{\Lambda}_b^{[n]}\right)^2 \times \left[\left(\mathbf{\Lambda}_{r,1}^{[n]}\mathbf{\Lambda}_f^{[n]}\right)^2 + \mathbf{I}_{N_b^{[n]}}\right]^{-1}\Bigg]^{-1}$$

where diagonal matrices $\mathbf{\Lambda}_{r,1}^{[n]}$ and $\mathbf{\Lambda}_{s,1}^{[n]}$ contain the largest $N_b^{[n]}$ singular values of $\mathbf{H}_{rd}^{[n]}$ and $\mathbf{H}_{sr}^{[n]}$, respectively. For Schur-convex objective functions, the relay and source matrices (18) and (20) diagonalize the channel up to a specific rotation of the source matrix.

Most practical linear nonregenerative multicarrier MIMO relay design problems can be solved by using the unified framework established by Theorem 1. For each objective function, we need to determine its Schur-convexity with respect to $\mathbf{d}\left[\mathbf{E}_0^{[n]}\left(\mathbf{B}^{[n]},\mathbf{F}^{[n]}\right)\right]$. The Schur-convexity results for most common objectives including MSE-based, SINR-based, and BER-based criteria are summarized in [21] for point-to-point MIMO systems. It is easy to find that these results can also be applied to the objective functions of linear nonregenerative multicarrier MIMO relay design. In the following two subsections, we demonstrate four examples of applying Theorem 1 and the Schur-convexity results in [21] to solve linear nonregenerative multicarrier MIMO relay design problems.

An interesting link between the transmitter optimization for point-to-point multicarrier MIMO communication systems [21] and our work can be drawn by rewriting the minimal MSE matrix (8). In fact, by using the matrix inversion lemma $(\mathbf{A} + \mathbf{BCD})^{-1} = \mathbf{A}^{-1} - \mathbf{A}^{-1}\mathbf{B}(\mathbf{DA}^{-1}\mathbf{B} + \mathbf{C}^{-1})^{-1}\mathbf{DA}^{-1}$, and the identity $\mathbf{B}^H(\mathbf{BCB}^H + \mathbf{I})^{-1}\mathbf{B} = \mathbf{C}^{-1} - (\mathbf{CB}^H\mathbf{BC} + \mathbf{C})^{-1}$ we have

$$\begin{aligned}
&\mathbf{E}_0^{[n]}\left(\mathbf{B}^{[n]},\mathbf{F}^{[n]}\right)\\
&= \mathbf{I}_{N_b^{[n]}} - \left(\bar{\mathbf{H}}^{[n]}\right)^H\left[\mathbf{H}_{rd}^{[n]}\mathbf{F}^{[n]}\mathbf{M}^{[n]}\left(\mathbf{H}_{rd}^{[n]}\mathbf{F}^{[n]}\right)^H + \mathbf{I}_{N_d}\right]^{-1}\bar{\mathbf{H}}^{[n]}\\
&= \mathbf{I}_{N_b^{[n]}} - \left(\mathbf{H}_{sr}^{[n]}\mathbf{B}^{[n]}\right)^H\Big[\left(\mathbf{M}^{[n]}\right)^{-1} - \Big(\mathbf{M}^{[n]}\left(\mathbf{H}_{rd}^{[n]}\mathbf{F}^{[n]}\right)^H \times \mathbf{H}_{rd}^{[n]}\mathbf{F}^{[n]}\mathbf{M}^{[n]} + \mathbf{M}^{[n]}\Big)^{-1}\Big]\mathbf{H}_{sr}^{[n]}\mathbf{B}^{[n]}\\
&= \mathbf{E}_1^{[n]}\left(\mathbf{B}^{[n]}\right) + \mathbf{E}_2^{[n]}\left(\mathbf{B}^{[n]},\mathbf{F}^{[n]}\right)
\end{aligned} \tag{21}$$

where

$$\begin{aligned}\mathbf{M}^{[n]} &\triangleq \mathbf{H}_{sr}^{[n]}\mathbf{B}^{[n]}\left(\mathbf{H}_{sr}^{[n]}\mathbf{B}^{[n]}\right)^H + \mathbf{I}_{N_r}\\ \mathbf{E}_1^{[n]}\left(\mathbf{B}^{[n]}\right) &= \left[\mathbf{I}_{N_b^{[n]}} + \left(\mathbf{H}_{sr}^{[n]}\mathbf{B}^{[n]}\right)^H\mathbf{H}_{sr}^{[n]}\mathbf{B}^{[n]}\right]^{-1} \quad (22)\\ \mathbf{E}_2^{[n]}\left(\mathbf{B}^{[n]},\mathbf{F}^{[n]}\right) &= \left(\mathbf{H}_{sr}^{[n]}\mathbf{B}^{[n]}\right)^H\left(\mathbf{M}^{[n]}\left(\mathbf{H}_{rd}^{[n]}\mathbf{F}^{[n]}\right)^H\right.\\ &\quad \left.\times \mathbf{H}_{rd}^{[n]}\mathbf{F}^{[n]}\mathbf{M}^{[n]} + \mathbf{M}^{[n]}\right)^{-1}\\ &\quad \times \mathbf{H}_{sr}^{[n]}\mathbf{B}^{[n]}. \quad (23)\end{aligned}$$

Obviously, $\mathbf{E}_1^{[n]}\left(\mathbf{B}^{[n]}\right)$ is the minimum MSE matrix for a point-to-point (one-hop) MIMO system. Thus, (21) indicates that the minimum MSE matrix for a two-hop linear nonregenerative MIMO relay system is a superposition of the minimum MSE matrix (22) for a point-to-point MIMO system and the increment of MSE (23) introduced by the relay-destination link. If the relay-destination link has a very high (infinite) channel gain, then $\mathbf{E}_2^{[n]}\left(\mathbf{B}^{[n]},\mathbf{F}^{[n]}\right) = \mathbf{0}_{N_b^{[n]}\times N_b^{[n]}}$, and $\mathbf{E}_0^{[n]}\left(\mathbf{B}^{[n]},\mathbf{F}^{[n]}\right) = \mathbf{E}_1^{[n]}\left(\mathbf{B}^{[n]}\right)$. Theorem 1 shows that for Schur-concave objective functions, the source matrix diagonalizes (22) as in [21]. When $\mathbf{H}_{rd}^{[n]}$ is finite, we know from (18) and (19) that the source and relay matrices jointly diagonalize (23). Therefore, our work is a generalization of the results in [21].

A. Relay Design With Schur-Concave Objective Functions

We consider the following three common design criteria with Schur-concave objective functions. The minimal arithmetic MSE (MA-MSE) relay [12], [13], [16] has the objective to minimize AMSE of the signal waveform estimation at all data streams (9). The maximal MI (MMI) relay [9]–[11], [15] aims to maximize the MI between source and destination in (11). While the maximal SINR (MSINR) relay has the goal to maximize the geometric product of the SINR of all data streams (12).

It can be shown similar to [21] that (9), (11), and (12) are all Schur-concave functions of vector $\mathbf{d}\left[\mathbf{E}_0^{[n]}\left(\mathbf{B}^{[n]},\mathbf{F}^{[n]}\right)\right]$. Thus, at each subcarrier, the optimal relay and source matrices have the structure specified by (18) and (19), respectively. We only needs to determine $\left\{\mathbf{\Lambda}_f^{[n]}\right\}$ and $\left\{\mathbf{\Lambda}_b^{[n]}\right\}$, which can be obtained by the following optimization problems. The objective function of the MA-MSE relay problem is given by

$$\min_{\left\{\lambda_{b,i}^{[n]}\right\},\left\{\lambda_{f,i}^{[n]}\right\}} \sum_{n=1}^{N_c}\sum_{i=1}^{N_b^{[n]}}\left(1+\frac{\left(\lambda_{r,i}^{[n]}\lambda_{f,i}^{[n]}\lambda_{s,i}^{[n]}\lambda_{b,i}^{[n]}\right)^2}{\left(\lambda_{r,i}^{[n]}\lambda_{f,i}^{[n]}\right)^2+1}\right)^{-1} \quad (24)$$

where $\lambda_{r,i}^{[n]}$, $\lambda_{f,i}^{[n]}$, $\lambda_{s,i}^{[n]}$, $\lambda_{b,i}^{[n]}$, $i=1,\ldots,N_b^{[n]}$, are the main diagonal elements of $\mathbf{\Lambda}_{r,1}^{[n]}$, $\mathbf{\Lambda}_f^{[n]}$, $\mathbf{\Lambda}_{s,1}^{[n]}$, $\mathbf{\Lambda}_b^{[n]}$, respectively, and for a scalar a, $\left\{a_i^{[n]}\right\} \triangleq \left\{a_1^{[1]},\ldots,a_{N_b^{[N_c]}}^{[N_c]}\right\}$. The objective of the MMI relay can be written as

$$\min_{\left\{\lambda_{b,i}^{[n]}\right\},\left\{\lambda_{f,i}^{[n]}\right\}} \sum_{n=1}^{N_c}\sum_{i=1}^{N_b^{[n]}}\log_2\left(1+\frac{\left(\lambda_{r,i}^{[n]}\lambda_{f,i}^{[n]}\lambda_{s,i}^{[n]}\lambda_{b,i}^{[n]}\right)^2}{\left(\lambda_{r,i}^{[n]}\lambda_{f,i}^{[n]}\right)^2+1}\right)^{-1}. \quad (25)$$

While for the MSINR relay design, the objective function is

$$\min_{\left\{\lambda_{b,i}^{[n]}\right\},\left\{\lambda_{f,i}^{[n]}\right\}} \prod_{n=1}^{N_c}\prod_{i=1}^{N_b^{[n]}}\frac{\left(\lambda_{r,i}^{[n]}\lambda_{f,i}^{[n]}\lambda_{s,i}^{[n]}\lambda_{b,i}^{[n]}\right)^2}{\left(\lambda_{r,i}^{[n]}\lambda_{f,i}^{[n]}\right)^2+1}. \quad (26)$$

All these three problems have the same transmission power constraints, given by

$$\text{s.t.}\quad \sum_{n=1}^{N_c}\sum_{i=1}^{N_b^{[n]}}\left(\lambda_{b,i}^{[n]}\right)^2 \le p_s \quad (27)$$

$$\sum_{n=1}^{N_c}\sum_{i=1}^{N_b^{[n]}}\left(\lambda_{f,i}^{[n]}\right)^2\left[\left(\lambda_{s,i}^{[n]}\lambda_{b,i}^{[n]}\right)^2+1\right] \le p_r \quad (28)$$

$$\lambda_{b,i}^{[n]} \ge 0,\ \ \lambda_{f,i}^{[n]} \ge 0,\ \ n=1,\ldots,N_c,\quad i=1,\ldots,N_b^{[n]}. \quad (29)$$

Closed-form solutions to problem (24), (27)–(29), problem (25), (27)–(29), and problem (26), (27)–(29) are intractable. In fact, since these problems are nonconvex, the global-optimal solution is hard to obtain. In [26], a grid search-based algorithm is designed to find the global-optimal solution for a multicarrier SISO relay system with the MMI criterion. In particular, at each subcarrier, the power loading parameters are obtained by solving a cubic equation with two fixed Lagrangian multipliers. A two-dimensional grid search is employed to find the optimal Lagrangian multipliers. Obviously, this algorithm can be extended to linear nonregenerative multicarrier MIMO relay systems, for example, to provide a global-optimal solution to problem (25), (27)–(29). However, the computational complexity of the algorithm in [26] is extremely high, since in order to obtain a reasonably good solution, search over a high-dense grid must be employed. The global-optimal power allocation parameters can also be obtained by using the dual decomposition technique [27]. However, similar to [26], a grid search must be performed to obtain the optimal dual variables. Therefore, the complexity of the dual decomposition technique is also very high.

In the following, we provide a numerical method to obtain a local-optimal $\left\{\lambda_{f,i}^{[n]}\right\}$ and $\left\{\lambda_{b,i}^{[n]}\right\}$ which has a much lower computational complexity than that of [26] and [27]. This method employs an alternating technique as shown in [11], [15], and [16]. To simplify notations, let us define

$$\begin{aligned}&a_i^{[n]} \triangleq \left(\lambda_{s,i}^{[n]}\right)^2,\quad b_i^{[n]} \triangleq \left(\lambda_{r,i}^{[n]}\right)^2,\\ &x_i^{[n]} \triangleq \left(\lambda_{b,i}^{[n]}\right)^2,\quad y_i^{[n]} \triangleq \left(\lambda_{f,i}^{[n]}\right)^2\left[\left(\lambda_{s,i}^{[n]}\lambda_{b,i}^{[n]}\right)^2+1\right],\\ &\qquad n=1,\ldots,N_c,\quad i=1,\ldots,N_b^{[n]}. \quad (30)\end{aligned}$$

Then the objective functions in (24)–(26) can be equivalently rewritten as (31)–(33), shown at the bottom of the next page. The transmission power constraints (27)–(29) are equivalently converted to

$$\text{s.t.}\quad \sum_{n=1}^{N_c}\sum_{i=1}^{N_b^{[n]}} x_i^{[n]} \le p_s \quad (34)$$

$$\sum_{n=1}^{N_c}\sum_{i=1}^{N_b^{[n]}} y_i^{[n]} \le p_r \tag{35}$$

$$x_i^{[n]} \ge 0, \quad y_i^{[n]} \ge 0, \quad n=1,\ldots,N_c, \quad i=1,\ldots,N_b^{[n]}. \tag{36}$$

From (31)–(36) we see that all three problems are symmetric in $\{x_i^{[n]}\}$ and $\{y_i^{[n]}\}$. Moreover, from (34)–(36) we find that the constraints on $\{x_i^{[n]}\}$ and $\{y_i^{[n]}\}$ are decomposed. Thus, we can efficiently update $\{x_i^{[n]}\}$ and $\{y_i^{[n]}\}$ in an alternating way [11], [15], [16]. As an example, for the MMI relay, with fixed $\{y_i^{[n]}\}$, we can update $\{x_i^{[n]}\}$ in (25) by solving

$$\min_{\{x_i^{[n]}\}} \sum_{n=1}^{N_c}\sum_{i=1}^{N_b^{[n]}} \log_2\left(\frac{a_i^{[n]}x_i^{[n]}+b_i^{[n]}y_i^{[n]}+1}{a_i^{[n]}b_i^{[n]}x_i^{[n]}y_i^{[n]}+a_i^{[n]}x_i^{[n]}+b_i^{[n]}y_i^{[n]}+1}\right) \tag{37}$$

$$\text{s.t.} \quad \sum_{n=1}^{N_c}\sum_{i=1}^{N_b^{[n]}} x_i^{[n]} \le p_s \tag{38}$$

$$x_i^{[n]} \ge 0, \quad n=1,\ldots,N_c, \quad i=1,\ldots,N_b^{[n]}. \tag{39}$$

Problem (37)–(39) has the well-known water-filling solution, given by

$$x_i^{[n]} = \frac{1}{2a_i^{[n]}}\left[\sqrt{\left(b_i^{[n]}y_i^{[n]}\right)^2+\frac{4a_i^{[n]}b_i^{[n]}y_i^{[n]}}{\mu_2}}-b_i^{[n]}y_i^{[n]}-2\right]^{\dagger}, \quad n=1,\ldots,N_c, \quad i=1,\ldots,N_b^{[n]}$$

where for a real-valued number x, $[x]^{\dagger} \triangleq \max(x,0)$. The water level μ_2 is the solution to the following nonlinear equation:

$$\sum_{n=1}^{N_c}\sum_{i=1}^{N_b^{[n]}} \frac{1}{a_i^{[n]}}\left[\sqrt{\left(b_i^{[n]}y_i^{[n]}\right)^2+\frac{4a_i^{[n]}b_i^{[n]}y_i^{[n]}}{\mu_2}}-b_i^{[n]}y_i^{[n]}-2\right]^{\dagger} = 2p_s$$

which can be efficiently solved by the bisection method [28]. Similarly, for the MA-MSE and MSINR relay design, we update $\{x_i^{[n]}\}$, respectively, as

$$x_i^{[n]} = \frac{1}{a_i^{[n]}}\left[\sqrt{\frac{a_i^{[n]}b_i^{[n]}y_i^{[n]}}{\mu_1\beta_i^{[n]}}}-1\right]^{\dagger}$$

$$x_i^{[n]} = \frac{1}{2a_i^{[n]}}\left[\sqrt{(\beta_i^{[n]})^2+\frac{4a_i^{[n]}\beta_i^{[n]}}{\mu_3}}-\beta_i^{[n]}\right]^{\dagger}, \quad n=1,\ldots,N_c, \quad i=1,\ldots,N_b^{[n]}$$

where $\beta_i^{[n]} \triangleq b_i^{[n]}y_i^{[n]}+1$, μ_1 and μ_3 are the solutions to the following equations, respectively:

$$\sum_{n=1}^{N_c}\sum_{i=1}^{N_b^{[n]}} \frac{1}{a_i^{[n]}}\left[\sqrt{\frac{a_i^{[n]}b_i^{[n]}y_i^{[n]}}{\mu_1\beta_i^{[n]}}}-1\right]^{\dagger} = p_s$$

$$\sum_{n=1}^{N_c}\sum_{i=1}^{N_b^{[n]}} \frac{1}{a_i^{[n]}}\left[\sqrt{(\beta_i^{[n]})^2+\frac{4a_i^{[n]}\beta_i^{[n]}}{\mu_3}}-\beta_i^{[n]}\right]^{\dagger} = 2p_s.$$

In a similar fashion, we can update $\{y_i^{[n]}\}$ with given $\{x_i^{[n]}\}$ for all three problems. Note that the conditional updates of $\{x_i^{[n]}\}$ and $\{y_i^{[n]}\}$ may either decrease or maintain but cannot increase the objective functions in (24)–(26). Monotonic convergence of $\{x_i^{[n]}\}$ and $\{y_i^{[n]}\}$ follows directly from this observation. After the convergence of the alternating algorithm, $\lambda_{b,i}^{[n]}$ and $\lambda_{f,i}^{[n]}$ can be obtained from (30) as

$$\lambda_{b,i}^{[n]} = \sqrt{x_i^{[n]}}, \quad \lambda_{f,i}^{[n]} = \sqrt{\frac{y_i^{[n]}}{\left(\lambda_{s,i}^{[n]}\right)^2 x_i^{[n]}+1}}, \quad n=1,\ldots,N_c, \quad i=1,\ldots,N_b^{[n]}. \tag{40}$$

Compared with [26] and [27], the alternating algorithm trades the local optimality for a greatly reduced computational complexity. Note that in [26] and [27], if the grid density is not sufficiently high, the global-optimal solution is not guaranteed. In Section IV, we study the performance comparison of [26] with our alternating algorithm through numerical simulations.

B. Relay Design With Schur-Convex Objective Functions

In multicarrier MIMO relay communication systems, the overall system performance, for example, the average raw BER, is dominated by the maximal MSE among all space-frequency data streams. The relay scheme which minimizes the maximal MSE (MM-MSE) has the following objective function:

$$\min_{\{\mathbf{B}^{[n]}\},\{\mathbf{F}^{[n]}\}} \max_{n,i} \left[\mathbf{E}_0^{[n]}\left(\mathbf{B}^{[n]},\mathbf{F}^{[n]}\right)\right]_{i,i}. \tag{41}$$

$$\min_{\{x_i^{[n]}\},\{y_i^{[n]}\}} \sum_{n=1}^{N_c}\sum_{i=1}^{N_b^{[n]}} \frac{a_i^{[n]}x_i^{[n]}+b_i^{[n]}y_i^{[n]}+1}{a_i^{[n]}b_i^{[n]}x_i^{[n]}y_i^{[n]}+a_i^{[n]}x_i^{[n]}+b_i^{[n]}y_i^{[n]}+1} \tag{31}$$

$$\min_{\{x_i^{[n]}\},\{y_i^{[n]}\}} \sum_{n=1}^{N_c}\sum_{i=1}^{N_b^{[n]}} \log_2\left(\frac{a_i^{[n]}x_i^{[n]}+b_i^{[n]}y_i^{[n]}+1}{a_i^{[n]}b_i^{[n]}x_i^{[n]}y_i^{[n]}+a_i^{[n]}x_i^{[n]}+b_i^{[n]}y_i^{[n]}+1}\right) \tag{32}$$

$$\min_{\{x_i^{[n]}\},\{y_i^{[n]}\}} \prod_{n=1}^{N_c}\prod_{i=1}^{N_b^{[n]}} \frac{a_i^{[n]}x_i^{[n]}+b_i^{[n]}y_i^{[n]}+1}{a_i^{[n]}b_i^{[n]}x_i^{[n]}y_i^{[n]}}. \tag{33}$$

It can be shown similar to [21] that (41) is a Schur-convex function of $\mathbf{d}\big[\mathbf{E}_0^{[n]}\big(\mathbf{B}^{[n]},\mathbf{F}^{[n]}\big)\big]$. Based on Theorem 1, the optimal structure of $\{\mathbf{F}^{[n]}\}$ and $\{\mathbf{B}^{[n]}\}$ are given by (18) and (20), respectively. Thus, we only need to optimize $\{\mathbf{\Lambda}_f^{[n]}\}$, $\{\mathbf{\Lambda}_b^{[n]}\}$, and $\{\mathbf{V}_b^{[n]}\}$. From Theorem 1 and Lemma 5 in the Appendix, we know that at each subcarrier, the elements of $\mathbf{d}\big[\mathbf{E}_0^{[n]}\big(\mathbf{B}^{[n]},\mathbf{F}^{[n]}\big)\big]$ should be identical for Schur-convex functions. Therefore, the objective function (41) can be written as

$$\min_{\left\{\mathbf{\Lambda}_b^{[n]}\right\},\left\{\mathbf{\Lambda}_f^{[n]}\right\}} \max_n \frac{1}{N_b^{[n]}}\operatorname{tr}\left(\mathbf{E}_0^{[n]}\big(\mathbf{\Lambda}_b^{[n]},\mathbf{\Lambda}_f^{[n]}\big)\right). \tag{42}$$

Function (42) can be equivalently converted to

$$\min_{\left\{\lambda_{b,i}^{[n]}\right\},\left\{\lambda_{f,i}^{[n]}\right\},t} \quad t \tag{43}$$

$$\text{s.t.}\quad t \geq \frac{1}{N_b^{[n]}}\sum_{i=1}^{N_b^{[n]}}\left(1+\frac{\big(\lambda_{r,i}^{[n]}\lambda_{f,i}^{[n]}\lambda_{s,i}^{[n]}\lambda_{b,i}^{[n]}\big)^2}{\big(\lambda_{r,i}^{[n]}\lambda_{f,i}^{[n]}\big)^2+1}\right)^{-1}, \quad n=1,\ldots,N_c. \tag{44}$$

Using simplified notations defined in (30), we can rewrite (43) and (44) as (45)–(46), shown at the bottom of the page. Finally, the MM-MSE relay design problem is given by (45), (46), and (34)–(36). This problem can be solved by using the alternating technique we developed in Section III-A. In particular, for fixed $\left\{y_i^{[n]}\right\}$, the solution of updating $\left\{x_i^{[n]}\right\}$ is given by

$$x_i^{[n]} = \frac{1}{a_i^{[n]}}\left[\sqrt{\frac{\nu^{[n]}a_i^{[n]}b_i^{[n]}y_i^{[n]}}{N_b^{[n]}\big(b_i^{[n]}y_i^{[n]}+1\big)}}-1\right]^{\dagger} \quad n=1,\ldots,N_c, \quad i=1,\ldots,N_b^{[n]}. \tag{47}$$

Equation (47) can be seen as a multilevel water-filling solution [21], where the water level at the nth subcarrier is determined by $\nu^{[n]}$. Obviously, $\nu^{[n]}$ should satisfy the constraint (46) at the nth subcarrier, while t is determined by the transmission power constraint (34) across all subcarriers. In practice, $\left\{x_i^{[n]}\right\}$ can be found by an algorithm with two bisection loops as listed in Table I.

Since $\left\{x_i^{[n]}\right\}$ and $\left\{y_i^{[n]}\right\}$ are symmetric in (45) and (46), $\left\{y_i^{[n]}\right\}$ can be updated in a similar fashion as $\left\{x_i^{[n]}\right\}$. A monotonic convergence of $\left\{x_i^{[n]}\right\}$ and $\left\{y_i^{[n]}\right\}$ is achieved because the conditional updates of $\left\{x_i^{[n]}\right\}$ and $\left\{y_i^{[n]}\right\}$ may either decrease or maintain but cannot increase the objective function (42). Finally, $\left\{\lambda_{b,i}^{[n]}\right\}$ and $\left\{\lambda_{f,i}^{[n]}\right\}$ are obtained by (40).

TABLE I
ALGORITHM 1: TWO BISECTION LOOPS IN COMPUTING $\left\{x_i^{[n]}\right\}$

1) Initialize the upper bound t_u and the lower bound t_l of t.
2) Set $t=(t_u+t_l)/2$.
   For each $n=1,\cdots,N_c$, applying the bisection method to solve the following equation for $\nu^{[n]}$, using (47) with given $\left\{y_i^{[n]}\right\}$.

$$\frac{1}{N_b^{[n]}}\sum_{i=1}^{N_b^{[n]}}\frac{a_i^{[n]}x_i^{[n]}+b_i^{[n]}y_i^{[n]}+1}{a_i^{[n]}b_i^{[n]}x_i^{[n]}y_i^{[n]}+a_i^{[n]}x_i^{[n]}+b_i^{[n]}y_i^{[n]}+1}=t$$

   Update $\left\{x_i^{[n]}\right\}$ as (47).
3) If $\left|\sum_{n=1}^{N_c}\sum_{i=1}^{N_b^{[n]}}x_i^{[n]}-p_s\right|\leq\epsilon$, then end; Here ϵ is a small positive number.
   elseif $\sum_{n=1}^{N_c}\sum_{i=1}^{N_b^{[n]}}x_i^{[n]}-p_s>\epsilon$, $t_l=t$, goto step 2.
   else $t_u=t$, goto step 2.

After $\mathbf{\Lambda}_f^{[n]}$ and $\mathbf{\Lambda}_b^{[n]}$ are obtained, the final step is to compute the rotation matrix $\mathbf{V}_b^{[n]}$ such that the main diagonal elements of

$$\big(\mathbf{V}_b^{[n]}\big)^T\left[\mathbf{I}_{N_b^{[n]}}+\big(\mathbf{\Lambda}_{r,1}^{[n]}\mathbf{\Lambda}_f^{[n]}\mathbf{\Lambda}_{s,1}^{[n]}\mathbf{\Lambda}_b^{[n]}\big)^2 \times\left[\big(\mathbf{\Lambda}_{r,1}^{[n]}\mathbf{\Lambda}_f^{[n]}\big)^2+\mathbf{I}_{N_b^{[n]}}\right]^{-1}\right]^{-1}\mathbf{V}_b^{[n]}$$

are identical. Such $\mathbf{V}_b^{[n]}$ can be any rotation matrix that satisfies $\left|\big[\mathbf{V}_b^{[n]}\big]_{i,k}\right|=\left|\big[\mathbf{V}_b^{[n]}\big]_{i,l}\right|, \forall i,k,l$. When the dimensions are appropriate such as a power of two, the discrete Fourier transform matrix can be chosen for $\mathbf{V}_b^{[n]}$. While for general case, $\mathbf{V}_b^{[n]}$ can be computed using the method developed in [29].

C. Subcarrier-Cooperative MIMO Relay System

In this subsection, we derive the optimal structure of $\mathbf{F}$ and $\mathbf{B}$ for a subcarrier-cooperative MIMO relay system. Based on the block-diagonal structure of (4) and (5) we can write the SVD of $\mathbf{H}_{sr}$ and $\mathbf{H}_{rd}$ as

$$\mathbf{H}_{sr}=\mathbf{U}_s\mathbf{\Lambda}_s\mathbf{V}_s^H \tag{48}$$
$$\mathbf{H}_{rd}=\mathbf{U}_r\mathbf{\Lambda}_r\mathbf{V}_r^H \tag{49}$$

where

$$\begin{aligned}
\mathbf{U}_s&=\operatorname{bd}\big(\mathbf{U}_s^{[1]},\mathbf{U}_s^{[2]},\ldots,\mathbf{U}_s^{[N_c]}\big)\\
\mathbf{\Lambda}_s&=\operatorname{bd}\big(\mathbf{\Lambda}_s^{[1]},\mathbf{\Lambda}_s^{[2]},\ldots,\mathbf{\Lambda}_s^{[N_c]}\big)\\
\mathbf{V}_s&=\operatorname{bd}\big(\mathbf{V}_s^{[1]},\mathbf{V}_s^{[2]},\ldots,\mathbf{V}_s^{[N_c]}\big)\\
\mathbf{U}_r&=\operatorname{bd}\big(\mathbf{U}_r^{[1]},\mathbf{U}_r^{[2]},\ldots,\mathbf{U}_r^{[N_c]}\big)\\
\mathbf{\Lambda}_r&=\operatorname{bd}\big(\mathbf{\Lambda}_r^{[1]},\mathbf{\Lambda}_r^{[2]},\ldots,\mathbf{\Lambda}_r^{[N_c]}\big)\\
\mathbf{V}_r&=\operatorname{bd}\big(\mathbf{V}_r^{[1]},\mathbf{V}_r^{[2]},\ldots,\mathbf{V}_r^{[N_c]}\big).
\end{aligned}$$

$$\min_{\left\{x_i^{[n]}\right\},\left\{y_{n,i}^{[n]}\right\},t} \quad t \tag{45}$$

$$\text{s.t.}\quad t\geq\frac{1}{N_b^{[n]}}\sum_{i=1}^{N_b^{[n]}}\frac{a_i^{[n]}x_i^{[n]}+b_i^{[n]}y_i^{[n]}+1}{a_i^{[n]}b_i^{[n]}x_i^{[n]}y_i^{[n]}+a_i^{[n]}x_i^{[n]}+b_i^{[n]}y_i^{[n]}+1}, \quad n=1,\ldots,N_c. \tag{46}$$

Note that although the main diagonal elements of $\mathbf{\Lambda}_s^{[n]}$ and $\mathbf{\Lambda}_f^{[n]}$, $n = 1, \ldots, N_c$, are ordered, the main diagonal elements of $\mathbf{\Lambda}_s$ and $\mathbf{\Lambda}_r$ remain unsorted. Let us introduce permutation matrices $\mathbf{\Pi}_{s,1}, \mathbf{\Pi}_{s,2}, \mathbf{\Pi}_{r,1}$, and $\mathbf{\Pi}_{r,2}$ with commensurate dimensions such that main diagonal elements of $\tilde{\mathbf{\Lambda}}_s \triangleq \mathbf{\Pi}_{s,1}\mathbf{\Lambda}_s\mathbf{\Pi}_{s,2}$ and $\tilde{\mathbf{\Lambda}}_r \triangleq \mathbf{\Pi}_{r,1}\mathbf{\Lambda}_r\mathbf{\Pi}_{r,2}$ are sorted in an increasing order, respectively. We can rewrite (48) and (49) as

$$\mathbf{H}_{sr} = \tilde{\mathbf{U}}_s\tilde{\mathbf{\Lambda}}_s\tilde{\mathbf{V}}_s^H, \quad \mathbf{H}_{rd} = \tilde{\mathbf{U}}_r\tilde{\mathbf{\Lambda}}_r\tilde{\mathbf{V}}_r^H$$

where $\tilde{\mathbf{U}}_s \triangleq \mathbf{U}_s\mathbf{\Pi}_{s,1}^T$, $\tilde{\mathbf{V}}_s \triangleq \mathbf{V}_s\mathbf{\Pi}_{s,2}$, $\tilde{\mathbf{U}}_r \triangleq \mathbf{U}_r\mathbf{\Pi}_{r,1}^T$, and $\tilde{\mathbf{V}}_r \triangleq \mathbf{V}_r\mathbf{\Pi}_{r,2}$.

According to Theorem 1, for Schur-concave objective functions, the optimal $\mathbf{F}$ and $\mathbf{B}$ jointly diagonalize the "super" source-relay-destination channel. Therefore, their optimal structure is given respectively by

$$\mathbf{F} = \tilde{\mathbf{V}}_{r,1}\mathbf{\Lambda}_f\tilde{\mathbf{U}}_{s,1}^H, \quad \mathbf{B} = \tilde{\mathbf{V}}_{s,1}\mathbf{\Lambda}_b \tag{50}$$

where $\mathbf{\Lambda}_f$ and $\mathbf{\Lambda}_b$ are $L \times L$ diagonal matrices, $\tilde{\mathbf{V}}_{r,1}$, $\tilde{\mathbf{U}}_{s,1}$, and $\tilde{\mathbf{V}}_{s,1}$ contain the rightmost L columns from $\tilde{\mathbf{V}}_r$, $\tilde{\mathbf{U}}_s$, and $\tilde{\mathbf{V}}_s$, respectively. For Schur-convex objective, the optimal structure can be written as

$$\mathbf{F} = \tilde{\mathbf{V}}_{r,1}\mathbf{\Lambda}_f\tilde{\mathbf{U}}_{s,1}^H, \quad \mathbf{B} = \tilde{\mathbf{V}}_{s,1}\mathbf{\Lambda}_b\mathbf{V}_b \tag{51}$$

where $\mathbf{V}_b$ is an $L \times L$ unitary rotation matrix.

From (50) and (51) we find that the cooperation among subcarriers is essentially carried out by the permutation matrices $\mathbf{\Pi}_{s,1}, \mathbf{\Pi}_{s,2}, \mathbf{\Pi}_{r,1}$, and $\mathbf{\Pi}_{r,2}$. In fact, the subcarriers are reshuffled at the relay and source nodes such that the strong space-frequency subchannels at the source-relay link are paired with the strong subchannels at the relay-destination link, while the weak subchannels are coupled with weak ones. The optimality of such pairing has been shown in [15] and [26] for the special case where the design objective is to maximize the MI between source and destination. Here we generalize this result to any problem with Schur-concave and/or Schur-convex objective functions.

After the optimal structure of $\mathbf{F}$ and $\mathbf{B}$ is determined, we are left with the optimization of $\mathbf{\Lambda}_f$ and $\mathbf{\Lambda}_b$, which can be efficiently solved by the alternating power loading algorithms developed in Sections III-A and III-B for Schur-concave and Schur-convex objective functions, respectively.

From the computational complexity point of view, performing SVD and calculating the power loading parameters are the two most computationally intensive parts of the proposed algorithm. By exploiting the block-diagonal feature of $\mathbf{F}$ and $\mathbf{B}$, the complexity of SVD for the subcarrier-cooperative system is equivalent to that of the subcarrier-independent system. However, since for a subcarrier-independent system, optimization of power loading parameters are decomposed into N_c subproblems, thus it has a lower computational complexity than the subcarrier-cooperative system. On the other hand, as mentioned in Section II-B, the subcarrier-cooperative relay system has a better performance than the subcarrier independent one. Such a performance-complexity tradeoff is very useful for practical systems and is further studied in Section IV.

TABLE II
CHARACTERISTICS OF THE ETSI "VEHICULAR A" CHANNEL ENVIRONMENT

Tap	Time Delays (T)	Average Power (dB)
1	0	0
2	1.55	-1
3	3.55	-9
4	5.45	-10
5	8.65	-15
6	12.55	-20

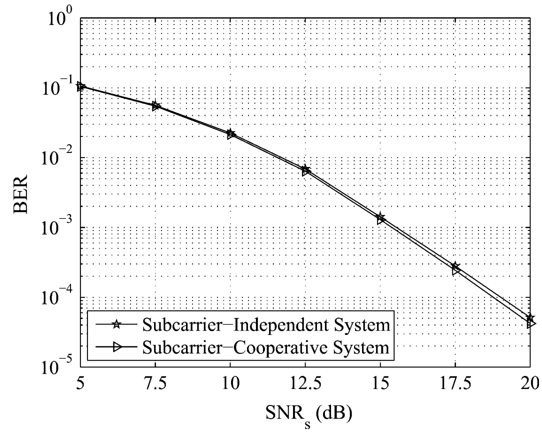

Fig. 1. Example 1: BER versus $\mathrm{SNR_s}$. $N_s = N_r = N_d = 3$, $N_b^{[n]} = 2$, $\mathrm{SNR_r} = 20$ dB.

IV. SIMULATIONS

In this section, we study the performance of the linear nonregenerative multicarrier MIMO relay techniques developed using the proposed framework through numerical simulations. For all examples, the channel between each transmit-receive antenna pair is modelled as the ETSI "Vehicular A" multipath channel environment which has been defined for the evaluation of UMTS radio interface proposals [30]. The multipath time delays and the variances of the multipath gains of the "Vehicular A" channel are shown in Table II, where T is the sampling interval.

An OFDM communication system with $N_c = 64$ subcarriers and QPSK constellations is assumed. The channel matrices have zero-mean entries with variances σ_s^2/N_s and σ_r^2/N_r for $\mathbf{H}_{sr}^{[n]}$ and $\mathbf{H}_{rd}^{[n]}$, respectively. We define

$$\mathrm{SNR_s} \triangleq \frac{\sigma_s^2 p_s N_r}{N_c N_s}, \quad \mathrm{SNR_r} \triangleq \frac{\sigma_r^2 p_r N_d}{N_c N_r}$$

as the SNR of the source-relay and relay-destination links, respectively. All simulation results are averaged over 2000 independent channel realizations.

First we compare the performance of the subcarrier-cooperative and subcarrier-independent systems, in order to study the performance-complexity tradeoffs of the former system. Fig. 1 shows the performance of both systems in terms of BER versus $\mathrm{SNR_s}$. Here we set $N_s = N_r = N_d = 3$, $N_b^{[n]} = 2, n = 1, \ldots, N_c$, and $\mathrm{SNR_r} = 20$ dB. Both systems are designed by using the proposed framework under the MA-MSE criterion. In particular, the subcarrier-independent system is optimized based on Section III-A, while the subcarrier-cooperative system is developed following the steps in Section III-C. From Fig. 1,

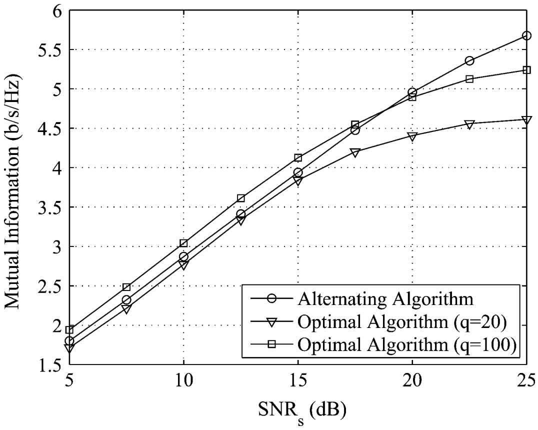

Fig. 2. Example 2: MI versus $\mathrm{SNR_s}$. $N_s = N_r = N_d = N_b^{[n]} = 1, \mathrm{SNR_r} =$ 20 dB.

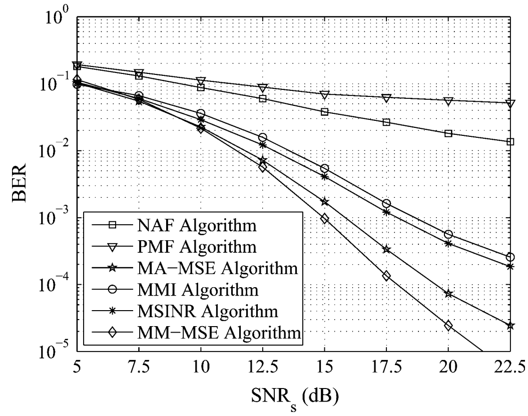

Fig. 3. Example 3: BER versus $\mathrm{SNR_s}$. $N_s = N_r = N_d = 3, N_b^{[n]} = 2$, $\mathrm{SNR_r} = 20$ dB.

we find that the subcarrier-cooperative system provides only a marginal performance improvement over the subcarrier-independent system. The reason can be explained as follows. The performance gain of the subcarrier-cooperative system is essentially obtained by pairing all space-frequency subchannels in a proper order. We call such gain space-frequency pairing gain. While in subcarrier-independent systems, only the spatial subchannels within one subcarrier is properly paired. It appears that such space-only pairing gain is only slightly smaller than the space-frequency pairing gain. Since the subcarrier-independent systems trade only a slight performance loss for a much reduced computational complexity, it is very attractive for practical applications. Therefore, in the following simulations, we focus on subcarrier-independent systems.

In the second example, we compare the proposed alternating power loading algorithm for Schur-concave objective functions developed in Section III-A with the optimal power loading algorithm proposed in [26]. Since [26] is designed for the MMI criteria, in Fig. 2, we show the performance of both algorithms in terms of MI versus $\mathrm{SNR_s}$. Here we set $N_s = N_r = N_d = 1$ (i.e., a SISO relay system as in [26]) and $\mathrm{SNR_r} = 20$ dB. To find the optimal solution, a two-dimensional grid search is performed as proposed in [26]. In particular, we try $q = 20$ and $q = 100$, respectively, where q denotes the number of uniformly-spaced intervals in each search dimension. From Fig. 2 we find that, as expected, the performance of [26] greatly depends on the density of the two-dimensional grid. When the grid is sparse, the global optimality is not guaranteed. In fact, at $q = 20$, it has a worse performance than our alternating algorithm throughout the whole $\mathrm{SNR_s}$ region. On the other hand, with a dense grid ($q = 100$), its performance is better than the proposed alternating algorithm in the low and medium $\mathrm{SNR_s}$ range. However, its performance is still inferior to that of our alternating algorithm at high $\mathrm{SNR_s}$. This indicates that a grid search with very high density (for example, $q = 1000$) is required at high $\mathrm{SNR_s}$. Obviously, the computational complexity for searching over a dense grid is extremely high. Therefore, for practical systems, the alternating power loading algorithm is a better choice.

In the following two examples, we compare the performance of different algorithms in terms of BER. We consider the MA-MSE, MMI, MSINR, and MM-MSE relay algorithms developed using the proposed framework, and the following two suboptimal schemes.

- Naive amplify-and-forward (NAF) algorithm: In this scheme, one chooses the following source matrix:

$$\mathbf{B}^{[n]} = \sqrt{\frac{p_s}{\sum_{n=1}^{N_c} N_b^{[n]}}} \times \left[\mathbf{I}_{N_b^{[n]}} \quad \mathbf{0}_{N_b^{[n]} \times (N_s - N_b^{[n]})}\right]^T, \quad n = 1, \ldots, N_c \tag{52}$$

  where $\mathbf{0}_{p\times m}$ stands for a $p\times m$ matrix with all zeros entries. The relay matrix $\mathbf{F}^{[n]}$ is taken as

$$\mathbf{F}^{[n]} = \sqrt{\frac{p_r}{N_c \mathrm{tr}(\boldsymbol{\Upsilon}^{[n]})}} \mathbf{I}_{N_r}, \quad n = 1, \ldots, N_c$$

  where

$$\boldsymbol{\Upsilon}^{[n]} = \mathbf{H}_{sr}^{[n]}\mathbf{B}^{[n]}\left(\mathbf{H}_{sr}^{[n]}\mathbf{B}^{[n]}\right)^H + \mathbf{I}_{N_r}, \ n = 1, \ldots, N_c.$$

- Pseudo match-and-forward (PMF) algorithm [31]: In this scheme, $\mathbf{B}^{[n]}$ is given by (52), and $\mathbf{F}^{[n]}$ is

$$\mathbf{F}^{[n]} = \sqrt{\frac{p_r}{N_c \mathrm{tr}\left(\left(\mathbf{H}_{sr}^{[n]}\mathbf{H}_{rd}^{[n]}\right)^H \boldsymbol{\Upsilon}^{[n]} \mathbf{H}_{sr}^{[n]}\mathbf{H}_{rd}^{[n]}\right)}} \times \left(\mathbf{H}_{sr}^{[n]}\mathbf{H}_{rd}^{[n]}\right)^H, \quad n = 1, \ldots, N_c.$$

In our third example, we choose $N_s = N_r = N_d = 3$, and $N_b^{[n]} = 2, n = 1, \ldots, N_c$. Fig. 3 shows BERs of all algorithms versus $\mathrm{SNR_s}$ for $\mathrm{SNR_r} = 20$ dB. While Fig. 4 demonstrates BERs of all algorithms versus $\mathrm{SNR_r}$ for $\mathrm{SNR_s}$ fixed at 20 dB. It can be seen from Figs. 3 and 4 that the algorithms developed using the proposed framework perform consistently better than the NAF and PMF algorithms over the whole $\mathrm{SNR_s}$ and $\mathrm{SNR_r}$ range.

In the fourth example, we simulate a relay system with different number of antennas at each node. In particular, we set $N_s = 5$, $N_r = 6$, $N_d = 4$, and $N_b^{[n]} = 3, n = 1, \ldots, N_c$. The BERs of all algorithms except the PMF scheme versus $\mathrm{SNR_s}$ are displayed in Fig. 5 for a fixed $\mathrm{SNR_r}$ at 20 dB. Fig. 6 shows BERs of the competing algorithms with respect to $\mathrm{SNR_r}$ for

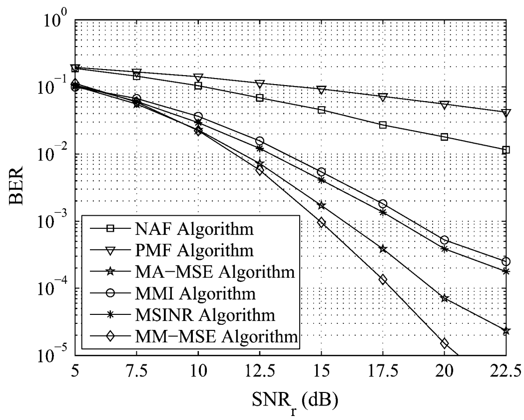

Fig. 4. Example 3: BER versus $\mathrm{SNR_r}$. $N_s = N_r = N_d = 3$, $N_b^{[n]} = 2$, $\mathrm{SNR_s} = 20$ dB.

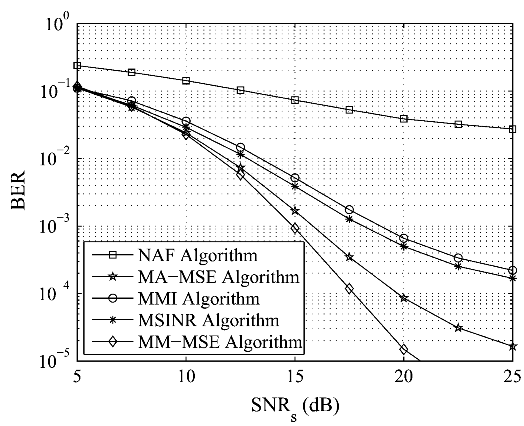

Fig. 5. Example 4: BER versus $\mathrm{SNR_s}$. $N_s = 5,\ N_r = 6,\ N_d = 4$, $N_b^{[n]} = 3$, $\mathrm{SNR_r} = 20$ dB.

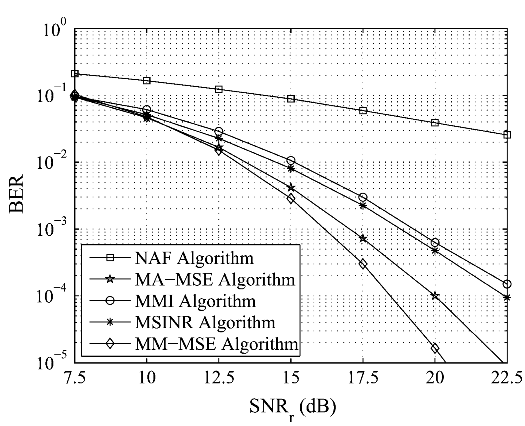

Fig. 6. Example 4: BER versus $\mathrm{SNR_r}$. $N_s = 5,\ N_r = 6,\ N_d = 4$, $N_b^{[n]} = 3$, $\mathrm{SNR_s} = 20$ dB.

$\mathrm{SNR_s} = 20$ dB. Note that in contrast to other schemes, the PMF algorithm requires $N_d = N_s$. We observe that the algorithms using our unified framework have a tremendously improved performance compared with the NAF algorithm.

From Figs. 3–6 we find that among the four algorithms developed using the proposed framework, the MM-MSE relay scheme has the best performance. Note that the MMI (as considered in [9]–[11] and [15]) is a good criterion only for coded systems in which the number of symbols for each coding block

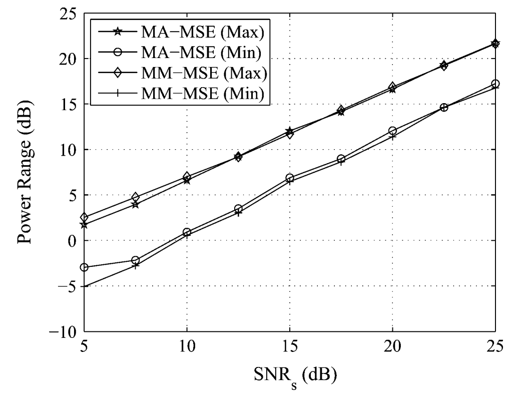

Fig. 7. Example 5: Power range versus $\mathrm{SNR_s}$. $N_s = N_r = N_d = 3$, $N_b^{[n]} = 2$, $\mathrm{SNR_r} = 20$ dB.

is large. However, in the numerical comparison, we consider uncoded systems with a small number of symbols (QPSK, $N_b^{[n]} = 2, 3$) for each block and compare the different schemes in term of raw BER. It is not surprising that the MMI-based algorithm does not yield a better performance than algorithms based on other criteria (such as MSE-based ones including MA-MSE and MM-MSE) in this setting.

In the last example, we investigate two practical issues of our algorithms: the dynamic range of the transmission power at each antenna, and the clipping probability at the source and relay nodes. The clipping probability is an important parameter for multicarrier systems and is defined as the probability that the instantaneous signal amplitude exceeds a clipping value. We choose MA-MSE and MM-MSE as the example of Schur-concave and Schur-convex objective functions, respectively. For both Schur-convex and Schur-concave objective functions, the transmission power $\rho_{s,k}$ and $\rho_{r,k}$ of the kth antenna at the source and relay nodes are computed respectively as

$$\rho_{s,k} = \sum_{n=1}^{N_c} \sum_{i=1}^{N_b^{[n]}} \left[\mathbf{B}_0^{[n]}\right]_{k,i}, \quad k = 1, \ldots, N_s$$

$$\rho_{r,k} = \sum_{n=1}^{N_c} \sum_{i=1}^{N_b^{[n]}} \left[\mathbf{F}_0^{[n]}\right]_{k,i}, \quad k = 1, \ldots, N_r.$$

We set $N_s = N_r = N_d = 3$, and $N_b^{[n]} = 2, n = 1, \ldots, N_c$. Fig. 7 shows the maximal and minimal transmission power of the first antenna $(k = 1)$ at the source node versus $\mathrm{SNR_s}$ at $\mathrm{SNR_r} = 20$ dB. Fig. 8 demonstrates the transmission power range of the first antenna at the relay node versus $\mathrm{SNR_r}$ for $\mathrm{SNR_s} = 20$ dB. From Figs. 7 and 8 we find that for a given $\mathrm{SNR_s}$ or $\mathrm{SNR_r}$, the required dynamic range of the power amplifier is around 5 dB, which can be easily implemented in practice. Interestingly, it can be seen from Figs. 7 and 8 that the MM-MSE algorithm yields a slightly larger dynamic power range than that of the MA-MSE algorithm.

The clipping probability at each antenna of the source and relay nodes is calculated respectively as

$$\Pr\left\{|S_s(t)| > \eta\sqrt{\frac{p_s}{N_s N_c}}\right\}$$

$$\Pr\left\{|S_r(t)| > \eta\sqrt{\frac{p_r}{N_r N_c}}\right\}$$

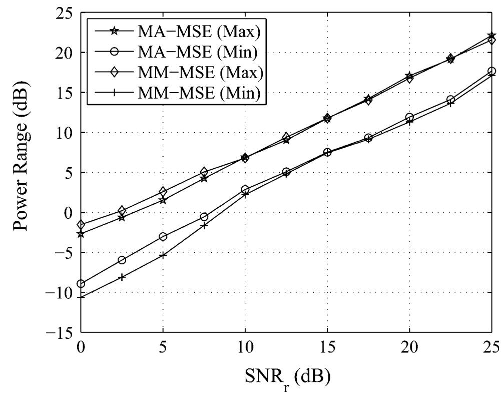

Fig. 8. Example 5: Power range versus $\mathrm{SNR_r}$. $N_s = N_r = N_d = 3$, $N_b^{[n]} = 2$, $\mathrm{SNR_s} = 20$ dB.

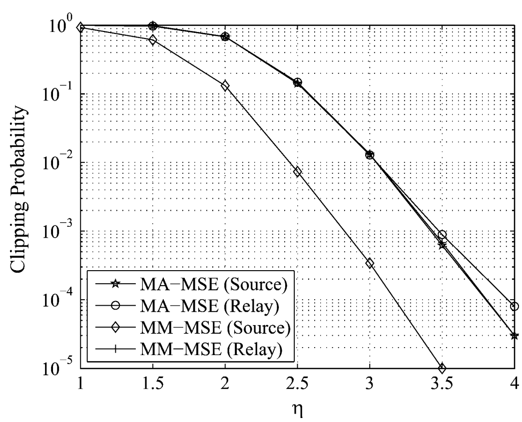

Fig. 9. Example 5: Clipping probability versus η. $N_s = N_r = N_d = 3$, $N_b^{[n]} = 2$, $\mathrm{SNR_s} = \mathrm{SNR_r} = 20$ dB.

where $\Pr\{\cdot\}$ stands for probability, $|S_s(t)|$ and $|S_r(t)|$ are the amplitude of the transmitted signal at the source and relay nodes, respectively, and η is a scalar controlling the clipping value. Fig. 9 shows the clipping probability versus η for $N_s = N_r = N_d = 3$, $N_b^{[n]} = 2$, $n = 1, \ldots, N_c$, and $\mathrm{SNR_s} = \mathrm{SNR_r} = 20$ dB. It can be seen from Fig. 9 that thanks to the rotation matrices $\mathbf{V}_b^{[n]}$, $n = 1, \ldots, N_c$, the clipping probability of the MM-MSE algorithm at the source node is much lower than that of the MA-MSE algorithm. We would like to mention that both the dynamic power range and the clipping probability can be controlled by incorporating additional constraints into the optimization problem [21]. From Figs. 3–6 and 9 we find that the MM-MSE algorithm has a better performance in terms of both BER and clipping probability than all competing techniques. Thus, it is very attractive for practical multicarrier MIMO relay systems.

V. Conclusion

We developed a unified framework which systematically solves most commonly formulated optimization problems for the source and relay matrices in a linear nonregenerative multicarrier MIMO relay communication system. We have shown that the optimal source and relay matrices jointly diagonalize the multicarrier MIMO relay channel if the objective function is Schur-concave. While for Schur-convex objective functions, the source-relay-destination channel is diagonalized after a specific rotation of the source matrix. With this optimal structure, the relay design problem is simplified to the issue of power loading among parallel SISO relay channels, and can be efficiently solved by using an alternating technique. Using the unified framework, we developed an MM-MSE relaying algorithm using a Schur-convex objective function. This new algorithm has a much better performance in terms of BER and clipping probability than all competing techniques.

Appendix
Proof of Theorem 1

To prove Theorem 1, we need the following lemmas from [19].

Lemma 1 [19, 9.B.1]: For a Hermitian matrix $\mathbf{A}$ with the vector of main diagonal elements $\mathbf{d}[\mathbf{A}]$ and the vector of eigenvalues $\boldsymbol{\lambda}[\mathbf{A}]$, there is $\mathbf{d}[\mathbf{A}] \prec \boldsymbol{\lambda}[\mathbf{A}]$.

Lemma 2 [19, Proof of 9.H.2]: For two $N \times N$ complex matrices $\mathbf{A}_1$ and $\mathbf{A}_2$, let $\mathbf{B} = \mathbf{A}_1^H \mathbf{A}_2 \mathbf{A}_1$, then $\boldsymbol{\sigma}_b \prec_{\mathrm{w}} (\boldsymbol{\sigma}_{a_1} \odot \boldsymbol{\sigma}_{a_2} \odot \boldsymbol{\sigma}_{a_1})$, where $\boldsymbol{\sigma}_b$, $\boldsymbol{\sigma}_{a_1}$ and $\boldsymbol{\sigma}_{a_2}$ denote $N \times 1$ vectors containing the singular values of $\mathbf{B}$, $\mathbf{A}_1$ and $\mathbf{A}_2$ arranged in the same order, respectively, and $\odot$ denotes the Schur (element-wise) product of two vectors.

Lemma 3 [19, 3.A.8]: A real-valued function f satisfies $\mathbf{x} \prec_{\mathbf{w}} \mathbf{y} \Rightarrow f(\mathbf{x}) \leq f(\mathbf{y})$ if and only if f is increasing and Schur-convex.

Lemma 4 [19, 9.H.1.h]: For two $N \times N$ positive semidefinite Hermitian matrices $\mathbf{A}$ and $\mathbf{B}$ with eigenvalues $\lambda_{a,i}$ and $\lambda_{b,i}$, $i = 1, \ldots, N$, arranged in the same order, respectively, there is $\mathrm{tr}(\mathbf{AB}) \geq \sum_{i=1}^{N} \lambda_{a,i}\lambda_{b,N+1-i}$.

Lemma 5 [19, p.7]: For an $N \times 1$ vector $\mathbf{x}$, let us define an $N \times 1$ vector $\mathbf{1}_{N\times 1}$ with identical elements of $\sum_{i=1}^{N} x_i/N$, there is $\mathbf{1}_{N\times 1} \prec \mathbf{x}$.

Lemma 6 [19, 9.B.2]: For any $N \times 1$ real-valued vector $\mathbf{x}$, there exists a real symmetric (and thus Hermitian) matrix $\mathbf{A}$ with equal main diagonal elements and eigenvalues given by $\mathbf{x}$. Equivalently, there is a unitary matrix $\mathbf{U}$ such that $\mathbf{A} = \mathbf{U}^H \mathcal{D}(\mathbf{x})\mathbf{U}$, where $\mathcal{D}(\mathbf{x})$ denotes a diagonal matrix taking $\mathbf{x}$ as the main diagonal.

We start to prove the first half of Theorem 1. Let us define

$$\begin{aligned} \mathbf{A}^{[n]} &\triangleq \mathbf{H}_{sr}^{[n]}\mathbf{B}^{[n]}(\mathbf{B}^{[n]})^H(\mathbf{H}_{sr}^{[n]})^H \\ &= \mathbf{U}_a^{[n]}\boldsymbol{\Lambda}_a^{[n]}(\mathbf{U}_a^{[n]})^H \end{aligned} \tag{53}$$

$$\begin{aligned} \mathbf{X}^{[n]} &\triangleq \mathbf{H}_{rd}^{[n]}\mathbf{F}^{[n]}(\mathbf{A}^{[n]} + \mathbf{I}_{N_r})^{1/2} \\ &= \mathbf{U}_x^{[n]}\boldsymbol{\Lambda}_x^{[n]}(\mathbf{V}_x^{[n]})^H \end{aligned} \tag{54}$$

where $\boldsymbol{\Lambda}_a^{[n]}$ is an $N_b^{[n]} \times N_b^{[n]}$ diagonal matrix containing nonzero eigenvalues of $\mathbf{A}^{[n]}$, $\mathbf{U}_a^{[n]}$ is an $N_r \times N_b^{[n]}$ matrix of the associated eigenvectors, $\mathbf{U}_x^{[n]}\boldsymbol{\Lambda}_x^{[n]}(\mathbf{V}_x^{[n]})^H$ is the SVD of $\mathbf{X}^{[n]}$ with the dimensions of $\mathbf{U}_x^{[n]}$, $\boldsymbol{\Lambda}_x^{[n]}$, $\mathbf{V}_x^{[n]}$ being $N_d \times N_b^{[n]}$, $N_b^{[n]} \times N_b^{[n]}$, $N_r \times N_b^{[n]}$, respectively. The diagonal elements of $\boldsymbol{\Lambda}_a^{[n]}$ and $\boldsymbol{\Lambda}_x^{[n]}$ are sorted in increasing order, respectively. Here, we use condition ii) in Theorem 1. From (53) and (54) we have

$$\mathbf{H}_{sr}^{[n]}\mathbf{B}^{[n]} = \mathbf{U}_a^{[n]}(\boldsymbol{\Lambda}_a^{[n]})^{1/2}\mathbf{Q}_1^{[n]} \tag{55}$$

$$\mathbf{H}_{rd}^{[n]}\mathbf{F}^{[n]} = \mathbf{X}^{[n]}\left(\mathbf{A}^{[n]} + \mathbf{I}_{N_r}\right)^{-1/2} \tag{56}$$

where $\mathbf{Q}_1^{[n]}$ is an arbitrary $N_b^{[n]} \times N_b^{[n]}$ unitary matrix. Substituting (55) and (56) into (8), we have

$$\begin{aligned}\mathbf{E}_0^{[n]} =& \mathbf{I}_{N_b^{[n]}} - \left(\bar{\mathbf{H}}^{[n]}\right)^H \Big[\mathbf{H}_{rd}^{[n]}\mathbf{F}^{[n]}(\mathbf{\Lambda}^{[n]} + \mathbf{I}_{N_r}) \\ & \times \left(\mathbf{H}_{rd}^{[n]}\mathbf{F}^{[n]}\right)^H + \mathbf{I}_{N_d}\Big]^{-1}\bar{\mathbf{H}}^{[n]} \\ =& \mathbf{I}_{N_b^{[n]}} - (\mathbf{H}_{sr}^{[n]}\mathbf{B}^{[n]})^H \\ & \times (\mathbf{A}^{[n]} + \mathbf{I}_{N_r})^{-1/2}(\mathbf{X}^{[n]})^H \\ & \times \left[\mathbf{X}^{[n]}(\mathbf{X}^{[n]})^H + \mathbf{I}_{N_d}\right]^{-1} \\ & \times \mathbf{X}^{[n]}(\mathbf{A}^{[n]} + \mathbf{I}_{N_r})^{-1/2}\mathbf{H}_{sr}^{[n]}\mathbf{B}^{[n]} \\ =& \mathbf{I}_{N_b^{[n]}} - (\mathbf{Q}_1^{[n]})^H(\mathbf{\Lambda}_a^{[n]})^{1/2} \\ & \times \left(\mathbf{\Lambda}_a^{[n]} + \mathbf{I}_{N_b^{[n]}}\right)^{-1/2}(\mathbf{U}_a^{[n]})^H \\ & \times \mathbf{V}_x^{[n]}\mathbf{\Lambda}_x^{[n]}\left[(\mathbf{\Lambda}_x^{[n]})^2 + \mathbf{I}_{N_b^{[n]}}\right]^{-1} \\ & \times \mathbf{\Lambda}_x^{[n]}(\mathbf{V}_x^{[n]})^H\mathbf{U}_a^{[n]} \\ & \times \left(\mathbf{\Lambda}_a^{[n]} + \mathbf{I}_{N_b^{[n]}}\right)^{-1/2}(\mathbf{\Lambda}_a^{[n]})^{1/2}\mathbf{Q}_1^{[n]} \\ =& \mathbf{I}_{N_b^{[n]}} - (\mathbf{Q}_1^{[n]})^H\mathbf{D}_1^{[n]}(\mathbf{Q}_2^{[n]})^H \\ & \times \mathbf{D}_2^{[n]}\mathbf{Q}_2^{[n]}\mathbf{D}_1^{[n]}\mathbf{Q}_1^{[n]} \\ \triangleq& \mathbf{I}_{N_b^{[n]}} - \mathbf{G}^{[n]}\end{aligned} \quad (57)$$

where the matrix inversion lemma is applied to obtain the first equation from (8), and

$$\begin{aligned}\mathbf{Q}_2^{[n]} &\triangleq (\mathbf{V}_x^{[n]})^H\mathbf{U}_a^{[n]} \\ \mathbf{D}_1^{[n]} &\triangleq \left[(\mathbf{\Lambda}_a^{[n]})^{-1} + \mathbf{I}_{N_b^{[n]}}\right]^{-1/2} \\ \mathbf{D}_2^{[n]} &\triangleq \left[(\mathbf{\Lambda}_x^{[n]})^{-2} + \mathbf{I}_{N_b^{[n]}}\right]^{-1}.\end{aligned}$$

It will be seen later that the power constraints (14) and (15) are invariant to $\mathbf{Q}_1^{[n]}$ and $\mathbf{Q}_2^{[n]}$.

Applying Lemmas 1 and 2 to $\mathbf{G}^{[n]}$ in (57), we have

$$\mathbf{d}\left[\mathbf{G}^{[n]}\right] \prec \boldsymbol{\lambda}\left[\mathbf{G}^{[n]}\right] \prec_{\mathrm{w}} \mathbf{d}\left[\left(\mathbf{D}_1^{[n]}\right)^2\mathbf{D}_2^{[n]}\right] \quad (58)$$

which indicates that $\mathbf{d}\left[\mathbf{G}^{[n]}\right]$ is majorized if

$$\mathbf{Q}_1^{[n]} = \mathbf{\Phi}_{N_b^{[n]}}, \quad \mathbf{Q}_2^{[n]} = \mathbf{\Phi}_{N_b^{[n]}}. \quad (59)$$

Here $\mathbf{\Phi}_m$ denotes an arbitrary $m \times m$ diagonal matrix with unit-norm main diagonal elements, i.e., $|[\mathbf{\Phi}_m]_{i,i}| = 1$, $[\mathbf{\Phi}_m]_{i,j} = 0, i,j = 1,\ldots,m, i \neq j$. Since $f\left(\mathbf{d}\left[\mathbf{E}_0^{[n]}\right]\right)$ is Schur-concave and increasing with respect to $\mathbf{d}\left[\mathbf{E}_0^{[n]}\right]$, $f\left(\mathbf{d}\left[\mathbf{I}_{N_b^{[n]}} - \mathbf{G}^{[n]}\right]\right)$ is Schur-concave and decreasing with respect to $\mathbf{d}\left[\mathbf{G}^{[n]}\right]$. Obviously, $-f\left(\mathbf{d}\left[\mathbf{I}_{N_b^{[n]}} - \mathbf{G}^{[n]}\right]\right)$ is Schur-convex and increasing with respect to $\mathbf{d}\left[\mathbf{G}^{[n]}\right]$. Based on (58) and Lemma 3, we have $-f\left(\mathbf{d}\left[\mathbf{I}_{N_b^{[n]}} - \mathbf{G}^{[n]}\right]\right) \leq -f\left(\mathbf{d}\left[\mathbf{I}_{N_b^{[n]}} - \left(\mathbf{D}_1^{[n]}\right)^2\mathbf{D}_2^{[n]}\right]\right)$, hence $f\left(\mathbf{d}\left[\mathbf{I}_{N_b^{[n]}} - \mathbf{G}^{[n]}\right]\right) \geq f\left(\mathbf{d}\left[\mathbf{I}_{N_b^{[n]}} - \left(\mathbf{D}_1^{[n]}\right)^2\mathbf{D}_2^{[n]}\right]\right)$, where the equality holds at (59). Without affecting the objective function (13) and the power constraints (14) and (15), we choose $\mathbf{Q}_1^{[n]} = \mathbf{Q}_2^{[n]} = \mathbf{I}_{N_b^{[n]}}$, hence $\mathbf{V}_x^{[n]} = \mathbf{U}_a^{[n]}$.

Now we consider the power constraints (14) and (15). Substituting the SVD of $\mathbf{H}_{sr}^{[n]}$ in (16) into (55), we have

$$\begin{aligned}&\begin{bmatrix}\mathbf{0}_{(N_r-r_1)\times(N_s-r_1)} & \mathbf{0}_{(N_r-r_1)\times r_1} \\ \mathbf{0}_{r_1\times(N_s-r_1)} & \mathbf{\Lambda}_{s,r_1}^{[n]}\end{bmatrix}\hat{\mathbf{B}}^{[n]} \\ &\qquad = (\mathbf{U}_s^{[n]})^H\mathbf{U}_a^{[n]}(\mathbf{\Lambda}_a^{[n]})^{1/2}\mathbf{Q}_1^{[n]}\end{aligned} \quad (60)$$

where $r_1 \triangleq \mathrm{rank}\left(\mathbf{H}_{sr}^{[n]}\right)$, $\mathbf{\Lambda}_{s,r_1}^{[n]}$ is a diagonal matrix containing all nonzero singular values of $\mathbf{H}_{sr}^{[n]}$, and $\hat{\mathbf{B}}^{[n]} \triangleq \left(\mathbf{V}_s^{[n]}\right)^H\mathbf{B}^{[n]}$. Let us denote $\mathbf{U}_s^{[n]} = \left[\mathbf{U}_{s,\bar{r}_1}^{[n]}, \mathbf{U}_{s,r_1}^{[n]}\right]$, where $\mathbf{U}_{s,\bar{r}_1}^{[n]}$ and $\mathbf{U}_{s,r_1}^{[n]}$ contain the vectors in $\mathbf{U}_s^{[n]}$ associated with the zero and nonzero singular values of $\mathbf{H}_{sr}^{[n]}$, respectively.

We find that depending on N_s, N_r, and r_1, (60) can be classified to the following three cases. Firstly, if $N_s = N_r = r_1$, (60) holds if and only if

$$\hat{\mathbf{B}}^{[n]} = \left(\mathbf{\Lambda}_{s,r_1}^{[n]}\right)^{-1}(\mathbf{U}_{s,r_1}^{[n]})^H\mathbf{U}_a^{[n]}(\mathbf{\Lambda}_a^{[n]})^{1/2}\mathbf{Q}_1^{[n]}. \quad (61)$$

Secondly, if $N_s > N_r = r_1$, then (60) is valid if and only if

$$\begin{bmatrix}\mathbf{0}_{r_1\times(N_s-r_1)} & \mathbf{\Lambda}_{s,r_1}^{[n]}\end{bmatrix}\hat{\mathbf{B}}^{[n]} = (\mathbf{U}_{s,r_1}^{[n]})^H\mathbf{U}_a^{[n]}(\mathbf{\Lambda}_a^{[n]})^{1/2}\mathbf{Q}_1^{[n]}. \quad (62)$$

Finally, if $N_s > r_1$ and $N_r > r_1$, (60) holds if and only if $\left(\mathbf{U}_{s,\bar{r}_1}^{[n]}\right)^H\mathbf{U}_a^{[n]} = \mathbf{0}_{(N_r-r_1)\times N_b^{[n]}}$ and (62) holds. For the latter two cases, the complete solution for $\hat{\mathbf{B}}^{[n]}$ is

$$\begin{aligned}\hat{\mathbf{B}}^{[n]} =& \begin{bmatrix}\mathbf{0}_{r_1\times(N_s-r_1)} & \left(\mathbf{\Lambda}_{s,r_1}^{[n]}\right)^{-1}\end{bmatrix}^H \\ &\times(\mathbf{U}_{s,r_1}^{[n]})^H\mathbf{U}_a^{[n]}(\mathbf{\Lambda}_a^{[n]})^{1/2}\mathbf{Q}_1^{[n]} + \begin{bmatrix}\mathbf{Z} & \mathbf{0}_{N_b^{[n]}\times r_1}\end{bmatrix}^H\end{aligned} \quad (63)$$

where $\mathbf{Z}$ is an arbitrary $N_b^{[n]} \times (N_s - r_1)$ matrix. Obviously, to minimize the transmission power at the source node, $\mathbf{Z}$ should be chosen as $\mathbf{0}_{N_b^{[n]}\times(N_s-r_1)}$. To determine $\mathbf{U}_a^{[n]}$ in (61) and (63), let us consider the transmission power at the $n\mathrm{th}$ subcarrier of the source node given by

$$\begin{aligned}\mathrm{tr}\left(\mathbf{B}^{[n]}(\mathbf{B}^{[n]})^H\right) =& \mathrm{tr}\left(\hat{\mathbf{B}}^{[n]}(\hat{\mathbf{B}}^{[n]})^H\right) \\ =& \mathrm{tr}\Big(\left(\mathbf{\Lambda}_{s,r_1}^{[n]}\right)^{-1}(\mathbf{U}_{s,r_1}^{[n]})^H\mathbf{U}_a^{[n]}\mathbf{\Lambda}_a^{[n]} \\ & \times(\mathbf{U}_a^{[n]})^H\mathbf{U}_{s,r_1}^{[n]}\left(\mathbf{\Lambda}_{s,r_1}^{[n]}\right)^{-1}\Big).\end{aligned} \quad (64)$$

Note that (64) is invariant to $\mathbf{Q}_1^{[n]}$ and $\mathbf{Q}_2^{[n]}$. It can be seen from Lemma 4 that (64) is minimized if $\mathbf{U}_a^{[n]} = \mathbf{U}_{s,1}^{[n]}\mathbf{\Phi}_{N_b^{[n]}}$. Without affecting the objective function and the constraints, we take $\mathbf{U}_a^{[n]} = \mathbf{U}_{s,1}^{[n]}$, and together with $\mathbf{Q}_1^{[n]} = \mathbf{I}_{N_b^{[n]}}$, we prove the optimal structure of $\mathbf{B}_0^{[n]}$ in (19) with $\mathbf{\Lambda}_b^{[n]} = \left(\mathbf{\Lambda}_{s,1}^{[n]}\right)^{-1}\left(\mathbf{\Lambda}_a^{[n]}\right)^{1/2}$.

Now we consider the power constraint (15). Similar to steps (60)–(63), by solving (56) for $\mathbf{F}^{[n]}$ we have $\left(\mathbf{U}_{r,\bar{r}_2}^{[n]}\right)^H\mathbf{U}_x^{[n]} = \mathbf{0}_{(N_d-r_2)\times N_b^{[n]}}$ if $N_d > r_2$ and

$$\begin{aligned}\hat{\mathbf{F}}^{[n]} =& \left(\mathbf{\Lambda}_{r,r_2}^{[n]}\right)^{-1}(\mathbf{U}_{r,r_2}^{[n]})^H\mathbf{U}_x^{[n]}\mathbf{\Lambda}_x^{[n]}\left(\mathbf{V}_x^{[n]}\right)^H \\ &\times\left(\mathbf{A}^{[n]} + \mathbf{I}_{N_r}\right)^{-1/2}, \quad N_r = r_2\end{aligned} \quad (65)$$

$$\hat{\mathbf{F}}^{[n]} = \left[\mathbf{0}_{r_2\times(N_r-r_2)} \quad \left(\mathbf{\Lambda}_{r,r_2}^{[n]}\right)^{-1}\right]^H \times (\mathbf{U}_{r,r_2}^{[n]})^H \mathbf{U}_x^{[n]} \mathbf{\Lambda}_x^{[n]} \left(\mathbf{V}_x^{[n]}\right)^H \times \left(\mathbf{A}^{[n]} + \mathbf{I}_{N_r}\right)^{-1/2}, \quad N_r > r_2 \tag{66}$$

where $r_2 \triangleq \mathrm{rank}\left(\mathbf{H}_{rd}^{[n]}\right)$, $\hat{\mathbf{F}}^{[n]} \triangleq \left(\mathbf{V}_r^{[n]}\right)^H \mathbf{F}^{[n]}$, $\mathbf{\Lambda}_{r,r_2}^{[n]}$ is a diagonal matrix containing all nonzero singular values of $\mathbf{H}_{rd}^{[n]}$, $\mathbf{U}_{r,\bar{r}_2}^{[n]}$ and $\mathbf{U}_{r,r_2}^{[n]}$ contain the vectors in $\mathbf{U}_r^{[n]}$ associated with the zero and nonzero singular values of $\mathbf{H}_{rd}^{[n]}$, respectively. To determine $\mathbf{U}_x^{[n]}$ in (65) and (66), we consider the power consumed by the relay node written as

$$\begin{aligned} &\mathrm{tr}\left(\mathbf{F}^{[n]}\left(\mathbf{A}^{[n]} + \mathbf{I}_{N_r}\right)\left(\mathbf{F}^{[n]}\right)^H\right) \\ &=\mathrm{tr}\left(\hat{\mathbf{F}}^{[n]}\left(\mathbf{A}^{[n]} + \mathbf{I}_{N_r}\right)\left(\hat{\mathbf{F}}^{[n]}\right)^H\right) \\ &=\mathrm{tr}\left(\left(\mathbf{\Lambda}_{r,r_2}^{[n]}\right)^{-1}(\mathbf{U}_{r,r_2}^{[n]})^H \mathbf{U}_x^{[n]} (\mathbf{\Lambda}_x^{[n]})^2 \left(\mathbf{U}_x^{[n]}\right)^H \right. \\ &\qquad \left. \times \mathbf{U}_{r,r_2}^{[n]} \left(\mathbf{\Lambda}_{r,r_2}^{[n]}\right)^{-1}\right). \end{aligned} \tag{67}$$

Obviously, (67) is invariant to $\mathbf{Q}_1^{[n]}$ and $\mathbf{Q}_2^{[n]}$. From Lemma 4, we know that (67) is minimized if $\mathbf{U}_x^{[n]} = \mathbf{U}_{r,1}^{[n]} \mathbf{\Phi}_{N_b^{[n]}}$. Without affecting the objective function and the constraints, we choose $\mathbf{U}_x^{[n]} = \mathbf{U}_{r,1}^{[n]}$, and using $\mathbf{V}_x^{[n]} = \mathbf{U}_a^{[n]} = \mathbf{U}_{s,1}^{[n]}$, we prove the optimal structure of $\mathbf{F}_0^{[n]}$ in (18) with $\mathbf{\Lambda}_f^{[n]} = \left(\mathbf{\Lambda}_{r,1}^{[n]}\right)^{-1} \mathbf{\Lambda}_x^{[n]} \left(\mathbf{\Lambda}_a^{[n]} + \mathbf{I}_{N_b^{[n]}}\right)^{-1/2}$. This concludes the proof for the first part of Theorem 1.

For Schur-convex objective functions, based on Definition 2 and Lemma 5, we know that the minimum of the objective function is obtained if $\mathbf{E}_0^{[n]}\left(\mathbf{B}^{[n]}, \mathbf{F}^{[n]}\right)$ has equal main diagonal elements. Let us introduce the eigendecomposition of $\left(\bar{\mathbf{H}}^{[n]}\right)^H \left(\bar{\mathbf{C}}^{[n]}\right)^{-1} \bar{\mathbf{H}}^{[n]} = \mathbf{U}_E^{[n]} \mathbf{\Lambda}_E^{[n]} \left(\mathbf{U}_E^{[n]}\right)^H$. Hence, we have $\mathbf{E}_0^{[n]}\left(\mathbf{B}^{[n]}, \mathbf{F}^{[n]}\right) = \mathbf{U}_E^{[n]}\left(\mathbf{I}_{N_b^{[n]}} + \mathbf{\Lambda}_E^{[n]}\right)^{-1}\left(\mathbf{U}_E^{[n]}\right)^H$. Based on Lemma 6, for any $\mathbf{B}^{[n]}$ and $\mathbf{F}^{[n]}$, we can improve the performance by using $\tilde{\mathbf{B}}^{[n]} = \mathbf{B}^{[n]} \mathbf{U}_E^{[n]} \mathbf{V}_b^{[n]}$ without affecting the power constraints (14) and (15). Here $\mathbf{V}_b^{[n]}$ is a unitary matrix such that $\mathbf{E}_0^{[n]}\left(\tilde{\mathbf{B}}^{[n]}, \mathbf{F}^{[n]}\right) = (\mathbf{V}_b^{[n]})^H \left(\mathbf{I}_{N_b^{[n]}} + \mathbf{\Lambda}_E^{[n]}\right)^{-1} \mathbf{V}_b^{[n]}$ has identical main diagonal elements, i.e.,

$$\left[\mathbf{E}_0^{[n]}\left(\tilde{\mathbf{B}}^{[n]}, \mathbf{F}^{[n]}\right)\right]_{i,i} = \frac{\mathrm{tr}\left(\mathbf{E}_0^{[n]}\left(\mathbf{B}^{[n]}, \mathbf{F}^{[n]}\right)\right)}{N_b^{[n]}} \quad i = 1, \ldots, N_b^{[n]}. \tag{68}$$

From (68), we see that $\mathbf{B}^{[n]}$ and $\mathbf{F}^{[n]}$ should be chosen to minimize $\mathrm{tr}\left(\mathbf{E}_0^{[n]}\left(\mathbf{B}^{[n]}, \mathbf{F}^{[n]}\right)\right)$. Such optimal $\mathbf{F}^{[n]}$ and $\mathbf{B}^{[n]}$ are given by (18) and (19), respectively, since $\mathrm{tr}\left(\mathbf{E}_0^{[n]}\left(\mathbf{B}^{[n]}, \mathbf{F}^{[n]}\right)\right)$ is a Schur-concave function of $\mathbf{d}\left[\mathbf{E}_0^{[n]}\left(\mathbf{B}^{[n]}, \mathbf{F}^{[n]}\right)\right]$.

In a nutshell, there are two steps in the optimal relay design with Schur-convex objectives. First, we calculate the optimal $\mathbf{F}_0^{[n]}$ and $\mathbf{B}_0^{[n]}$ according to (18), (19) and using $\mathrm{tr}\left(\mathbf{E}_0^{[n]}\left(\mathbf{B}^{[n]}, \mathbf{F}^{[n]}\right)\right)$ as the objective function. After the first step, we obtain a diagonal $\mathbf{E}_0^{[n]}\left(\mathbf{B}^{[n]}, \mathbf{F}^{[n]}\right)$ with minimal $\mathrm{tr}\left(\mathbf{E}_0^{[n]}\left(\mathbf{B}^{[n]}, \mathbf{F}^{[n]}\right)\right)$. In the second step, $\mathbf{B}_0^{[n]}$ is rotated by $\mathbf{V}_b^{[n]}$ based on (68). Therefore, for Schur-convex objective functions, $\mathbf{F}_0^{[n]}$ is given by (18), while $\mathbf{B}_0^{[n]}$ is represented as (20). $\square$

References

[1] E. C. van der Meulen, "Three-terminal communication channels," *Adv. Appl. Prob.*, vol. 3, pp. 120–154, 1971.

[2] T. M. Cover and A. A. El Gamal, "Capacity theorems for the relay channel," *IEEE Trans. Inf. Theory*, vol. 25, pp. 572–584, Sep. 1979.

[3] A. Sendonaris, E. Erkip, and B. Aazhang, "User cooperation diversity—Part I and Part II," *IEEE Trans. Commun.*, vol. 51, pp. 1927–1948, Nov. 2003.

[4] Y. Hua, Y. Mei, and Y. Chang, "Wireless antennas—making wireless communications perform like wireline communications," in *Proc. IEEE Topical Conf. Wireless Commun. Tech.*, Honolulu, HI, Oct. 15–17, 2003, pp. 1–27.

[5] J. N. Laneman, D. N. C. Tse, and G. W. Wornell, "Cooperative diversity in wireless networks: Efficient protocols and outage behavior," *IEEE Trans. Inf. Theory*, vol. 50, pp. 3062–3080, Dec. 2004.

[6] G. Kramer, M. Gastpar, and P. Gupta, "Cooperative strategies and capacity theorems for relay networks," *IEEE Trans. Inf. Theory*, vol. 51, pp. 3037–3063, Sep. 2005.

[7] B. Wang, J. Zhang, and A. Høst-Madsen, "On the capacity of MIMO relay channels," *IEEE Trans. Inf. Theory*, vol. 51, pp. 29–43, Jan. 2005.

[8] M. Yuksel and E. Erkip, "Multi-antenna cooperative wireless systems: A diversity multiplexing tradeoff perspective," *IEEE Trans. Inf. Theory*, vol. 53, pp. 3371–3393, Oct. 2007.

[9] X. Tang and Y. Hua, "Optimal design of non-regenerative MIMO wireless relays," *IEEE Trans. Wireless Commun.*, vol. 6, pp. 1398–1407, Apr. 2007.

[10] O. Muñoz-Medina, J. Vidal, and A. Agustín, "Linear transceiver design in nonregenerative relays with channel state information," *IEEE Trans. Signal Process.*, vol. 55, no. 6, pp. 2593–2604, Jun. 2007.

[11] Z. Fang, Y. Hua, and J. C. Koshy, "Joint source and relay optimization for a non-regenerative MIMO relay," in *Proc. IEEE Workshop Sensor Array Multi-Channel Signal Processing*, Waltham, WA, Jul. 2006, pp. 239–243.

[12] W. Guan and H. Luo, "Joint MMSE transceiver design in non-regenerative MIMO relay systems," *IEEE Commun. Lett.*, vol. 12, pp. 517–519, Jul. 2008.

[13] A. S. Behbahani, R. Merched, and A. M. Eltawil, "Optimizations of a MIMO relay network," *IEEE Trans. Signal Process.*, vol. 56, no. 10, pp. 5062–5073, Oct. 2008.

[14] Y. Fan and J. Thompson, "MIMO configurations for relay channels: Theory and practice," *IEEE Trans. Wireless Commun.*, vol. 6, pp. 1774–1786, May 2007.

[15] I. Hammerström and A. Wittneben, "Power allocation schemes for amplify-and-forward MIMO-OFDM relay links," *IEEE Trans. Wireless Commun.*, vol. 6, pp. 2798–2802, Aug. 2007.

[16] Y. Rong, "Non-regenerative multicarrier MIMO relay communications based on minimization of mean-squared error," in *Proc. IEEE Int. Conf. Commun.*, Dresden, Germany, Jun. 2009.

[17] B. Khoshnevis, W. Yu, and R. Adve, "Grassmannian beamforming for MIMO amplify-and-forward relaying," *IEEE J. Sel. Areas Commun.*, vol. 26, pp. 1397–1407, Oct. 2008.

[18] S. Peters and R. W. Heath, "Nonregenerative MIMO relaying with optimal transmit antenna selection," *IEEE Signal Process. Lett.*, vol. 15, pp. 421–424, 2008.

[19] A. W. Marshall and I. Olkin, *Inequalities: Theory of Majorization and Its Applications*. New York: Academic, 1979.

[20] T. Ando, "Majorization, doubly stochastic matrices, and comparison of eigenvalues," *Linear Algebra Appl.*, pp. 163–248, 1989.

[21] D. P. Palomar, J. M. Cioffi, and M. A. Lagunas, "Joint Tx-Rx beamforming design for multicarrier MIMO channels: A unified framework for convex optimization," *IEEE Trans. Signal Process.*, vol. 51, no. 9, pp. 2381–2401, Sep. 2003.

[22] S. Jafar and A. Goldsmith, "Transmitter optimization and optimality of beamforming for multiple antenna systems," *IEEE Trans. Wireless Commun.*, vol. 3, pp. 1165–1175, Jul. 2004.

[23] A. Soysal and S. Ulukus, "Optimum power allocation for single-user MIMO and multi-user MIMO-MAC with partial CSI," *IEEE J. Sel. Areas Commun.*, vol. 25, pp. 1402–1412, Sep. 2007.

[24] N. Fawaz, K. Zarifi, M. Debbah, and D. Gesbert, "Asymptotic capacity and optimal precoding strategy of multi-level precode & forward in correlated channels," in *Proc. IEEE Inf. Theory Workshop*, Porto, Portugal, May 2008, pp. 209–213.

[25] S. M. Kay, *Fundamentals of Statistical Signal Processing: Estimation Theory*. Englewood Cilffs, NJ: Prentice-Hall, 1993.

[26] W. Zhang, U. Mitra, and M. Chiang, "Optimization of amplify-and-forward multicarrier two-hop transmission," *IEEE Trans. Commun.*, submitted for publication.

[27] R. Cendrillon, W. Yu, M. Moonen, J. Verlinden, and T. Bostoen, "Optimal multiuser spectrum balancing for digital subscriber lines," *IEEE Trans. Commun.*, vol. 54, pp. 922–933, May 2006.

[28] S. Boyd and L. Vandenberghe, *Convex Optimization*. Cambridge, U.K.: Cambridge Univ. Press, 2004.

[29] P. Viswanath and V. Anantharam, "Optimal sequences and sum capacity of synchronous CDMA systems," *IEEE Trans. Inf. Theory*, vol. 45, pp. 1984–1993, Sep. 1999.

[30] *Universal Mobile Telecommunications System (UMTS); Selection Procedures for the Choice of Radio Transmission Technologies of the UMTS (UMTS 30.03 Version 3.2.0)*, ETSI Standard, Document TR 101 112 V3.2.0, 1998.

[31] P. U. Sripathi and J. S. Lehnert, "A throughput scaling law for a class of wireless relay networks," in *Proc. 38th Annu. Asilomar Conf. Signals, Systems, Computers*, Nov. 2004, vol. 2, pp. 1333–1337.

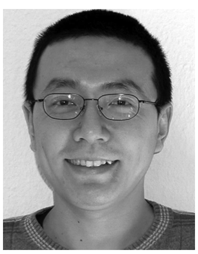

Yue Rong (S'03–M'06) received the B.E. degree from Shanghai Jiao Tong University, China, the M.Sc. degree from the University of Duisburg-Essen, Duisburg, Germany, and the Ph.D. degree (*summa cum laude*) from Darmstadt University of Technology, Darmstadt, Germany, all in electrical engineering, in 1999, 2002, and 2005, respectively.

From April 2001 to October 2001, he was a Research Assistant at the Fraunhofer Institute of Microelectronic Circuits and Systems, Duisburg, Germany. From October 2001 to March 2002, he was with Nokia Limited, Bochum, Germany. From November 2002 to March 2005, he was a Research Associate at the Department of Communication Systems in the University of Duisburg-Essen. From April 2005 to January 2006, he was a Research Associate with the Institute of Telecommunications at Darmstadt University of Technology. From February 2006 to November 2007, he was a Postdoctoral Researcher with the Department of Electrical Engineering, University of California, Riverside. Since December 2007, he has been a Lecturer with the Department of Electrical and Computer Engineering, Curtin University of Technology, Perth, Australia. His research interests include signal processing for communications, wireless communications, wireless networks, applications of linear algebra and optimization methods, and statistical and array signal processing.

Dr. Rong received the 2001–2002 Graduate Sponsoring Asia scholarship of DAAD/ABB (Germany) and the 2004 Chinese Government Award for Outstanding Self-Financed Students Abroad (China).

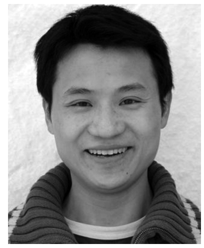

Xiaojun Tang (S'07) received the B.S. and M.S. degrees from University of Electronic Science and Technology of China (UESTC) in 2000 and 2003, respectively. He is now working toward the Ph.D. degree at Wireless Information Network Laboratory (WINLAB) at Rutgers University, New Brunswick, NJ.

From 2003 to 2005, he was a Research Assistant at the University of California, Riverside, working on MIMO cooperative and relay systems. Since 2005, he has been with WINLAB at Rutgers University working on information theoretic security and ensuring wireless security at the physical layer. In the summer of 2008, he was a research intern at DOCOMO Communications Laboratory USA. His research interests are in the areas of wireless communications, signal processing, information theory, modern coding theory, information privacy and security.

Mr Tang received an outstanding teaching assistant award at University of California, Riverside, in 2005, and multiple year research fellowships at Rutgers University. He also received a best student paper award at the IEEE VTC 2009, Anchorage, AK.

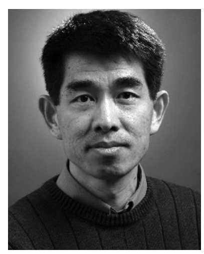

Yingbo Hua (S'86–M'88–SM'92–F'02) received the B.S. degree from Nanjing Institute of Technology, Nanjing, China, in February 1982, and M.S. and Ph.D. degrees from Syracuse University, Syracuse, NY, in 1983 and 1988, respectively.

From 1988 to 1989, he was a research fellow at Syracuse, consulting for Syracuse Research Co., NY, and Aeritalia Co., Italy. He was Lecturer from February 1990 to 1992, Senior Lecturer from 1993 to 1995, and Reader and Associate Professor from 1996 to 2001, with the University of Melbourne, Australia. He served as a visiting professor with Hong Kong University of Science and Technology from 1999 to 2000, and consulted for Microsoft Research Co., WA, during summer 2000. Since February 2001, he has been Professor of Electrical Engineering with the University of California, Riverside, CA. He is an author/coauthor of numerous articles in journals, conference proceedings and books, which span the fields of sensor array signal processing, channel and system identification, wireless communications and networking, and distributed computations in sensor networks. He is a co-editor of *Signal Processing Advances in Wireless and Mobile Communications*, Prentice-Hall, 2001, and *High-Resolution and Robust Signal Processing*, Marcel Dekker, 2003.

Prof. Hua has served on the Editorial Boards for IEEE TRANSACTIONS ON SIGNAL PROCESSING, IEEE SIGNAL PROCESSING LETTERS, *IEEE Signal Processing Magazine,* and *Signal Processing* (EURASIP). He also served on IEEE SPS Technical Committees for Underwater Acoustic Signal Processing, Sensor Array and Multichannel Signal Processing, and Signal Processing for Communications and Networking, and on numerous international conference organization committees.